Brain, Behavior, & Immunity - Health 4 (2020) 100057

Contents lists available at ScienceDirect

Brain, Behavior, & Immunity - Health

journal homepage: www.editorialmanager.com/bbih/default.aspx

Cranial irradiation acutely and persistently impairs injury-induced microglial proliferation

Elizabeth K. Belcher [a,b], Tara B. Sweet [a], Berke Karaahmet [a], Dawling A. Dionisio-Santos [a], Laura D. Owlett [a], Kimberly A. Leffler [a], Michelle C. Janelsins [a,b], Jacqueline P. Williams [c], John A. Olschowka [a], M. Kerry O'Banion [a,*]

[a] Department of Neuroscience, University of Rochester Medical Center, 601 Elmwood Ave, Box 603, Rochester, NY, 14642, USA
[b] Department of Surgery, University of Rochester Medical Center, 265 Crittenden Blvd, Box 658, Rochester, NY, 14642, USA
[c] Department of Environmental Medicine, University of Rochester Medical Center, 601 Elmwood Ave, Box EHSC, Rochester, NY, 14642, USA

ARTICLE INFO

Keywords:
Microglia
Proliferation
Radiation
Brain
Stab
Injury
Metastatic tumor
CSF1R

ABSTRACT

Microglia, the resident immune cells of the central nervous system (CNS), play multiple roles in maintaining CNS homeostasis and mediating tissue repair, including proliferating in response to brain injury and disease. Cranial irradiation (CI), used for the treatment of brain tumors, has a long-lasting anti-proliferative effect on a number of cell types in the brain, including oligodendrocyte progenitor and neural progenitor cells; however, the effect of CI on CNS-resident microglial proliferation is not well characterized. Using a sterile cortical needle stab injury model in mice, we found that the ability of CNS-resident microglia to proliferate in response to injury was impaired by prior CI, in a dose-dependent manner, and was nearly abolished by a 20 Gy dose. Similarly, in a metastatic tumor model, prior CI (20 Gy) reduced microglial proliferation in response to tumor growth. The effect of irradiation was long-lasting; 20 Gy CI 6 months prior to stab injury significantly impaired microglial proliferation. We also investigated how stab and/or irradiation impacted levels of P2Y12R, CD68, CSF1, IL-34 and CSF1R, factors involved in the brain's normal response to injury. P2Y12R, CD68, CSF1, and IL-34 expression were altered by stab similarly in irradiated mice and controls; however, CSF1R was differentially affected. qRT-PCR and flow cytometry analyses demonstrated that CI reduced overall *Csf1r* mRNA levels and microglial specific CSF1R protein expression, respectively. Interestingly, *Csf1r* mRNA levels increased after injury in unirradiated controls; however, *Csf1r* levels were persistently decreased in irradiated mice, and did not increase in response to stab. Together, our data demonstrate that CI leads to a significant and lasting impairment of microglial proliferation, possibly through a CSF1R-mediated mechanism.

1. Introduction

Cranial irradiation is used to treat as many as 92% of the 80,000 patients that are diagnosed each year in the United States with central nervous system (CNS) tumors (Boyle and Levin, 2008; Delaney et al., 2005; Ewend et al., 2005). By impairing cancer cell survival and mitosis, irradiation is effective at slowing the growth and spread of tumors. Unfortunately, cranial irradiation also impacts healthy cells in the brain, contributing to normal tissue injury. Indeed, the proliferation of oligodendrocyte precursor cells (OPCs) and neural progenitor cells (NPCs) is impaired for months after cranial irradiation in rodents (Begolly et al., 2018; Mizumatsu et al., 2003; Rola et al., 2004a; Sweet et al., 2014, 2016). Importantly, these effects on proliferation are associated with impairments in neural function and animal behavior (Rola et al., 2004b; Snyder et al., 2005) and may relate to the many side effects of cranial radiotherapy (Greene-Schloesser et al., 2013).

Microglia, often referred to as the tissue resident macrophages of the CNS, mediate CNS repair in many contexts of injury and disease. ATP released from damaged cells binds to the microglial specific receptor, P2Y12R, mediating microglial process extension towards the lesion,

* Corresponding author. Del Monte Institute for Neuroscience, 601 Elmwood Avenue, Box 603, Rochester, NY 14642, USA.
E-mail addresses: elizabeth_belcher@urmc.rochester.edu (E.K. Belcher), tsweet@brockport.edu (T.B. Sweet), berke_karaahmet@urmc.rochester.edu (B. Karaahmet), dawling_dionisiosantos@urmc.rochester.edu (D.A. Dionisio-Santos), laura_owlett@urmc.rochester.edu (L.D. Owlett), kimberly_leffler@urmc.rochester.edu (K.A. Leffler), michelle_janelsins@urmc.rochester.edu (M.C. Janelsins), jackie_williams@urmc.rochester.edu (J.P. Williams), john_olschowka@urmc.rochester.edu (J.A. Olschowka), kerry_obanion@urmc.rochester.edu (M.K. O'Banion).

https://doi.org/10.1016/j.bbih.2020.100057
Received 6 January 2020; Received in revised form 28 February 2020; Accepted 1 March 2020
Available online 6 March 2020

which may help restore the blood brain barrier (Davalos et al., 2005; Lou et al., 2016; Swiatkowski et al., 2016). Additionally, microglia proliferate robustly at sites of brain injury, contributing to a glial scar and isolating peripheral immune cell infiltration to the wounded area (Bellver-Landete et al., 2019; Lalancette-Hebert et al., 2007; Leibovich and Ross, 1975). Proliferation may also serve to increase the number of microglia available for mounting and resolving inflammation and phagocytosing dead cells and debris (Tremblay et al., 2011). Although postnatal expansion of the microglial population was previously thought to occur through the infiltration of circulating monocytes, it is now known that proliferation of CNS-resident microglia is largely responsible for increased microglial numbers after CNS injury (Ajami et al., 2007; Mildner et al., 2007).

Key signals that induce and regulate microglial proliferation include colony stimulating factor 1 (CSF1) and interleukin 34 (IL-34), which are expressed by a variety of cell types in the brain (Gomez-Nicola et al., 2013; Greter et al., 2012; Masteller and Wong, 2014; Mizuno et al., 2011; Wang and Colonna, 2014; Yamamoto et al., 2012; Zhang et al., 2014). Both ligands bind the CSF1 receptor (CSF1R), which, in the CNS, is primarily present on microglia (Chihara et al., 2010; Raivich et al., 1998). When CNS tissue is injured, neurons and microglia upregulate CSF1, which leads to microglial proliferation by binding CSF1R (Guan et al., 2016; Okubo et al., 2016; Raivich et al., 1998; Takeuchi et al., 2001; Yamamoto et al., 2010). Indeed, either absence of CSF1 or pharmacological inhibition of CSF1R prevents microglial proliferation after injury (Berezovskaya et al., 1995; Okubo et al., 2016; Raivich et al., 1994). Additionally, alterations in CSF1, IL-34 and CSF1R expression can induce or prevent microglial proliferation in various disease and injury models (Gomez-Nicola et al., 2013; Okubo et al., 2016; Raivich et al., 1998; Yamamoto et al., 2010). While studies have demonstrated that irradiation increases tumor CSF1 expression (Xu et al., 2013), to our knowledge, none have investigated whether cranial irradiation alters CSF1R, CSF1 and IL-34 expression in normal tissues of the brain.

A number of studies have investigated the effects of cranial irradiation on microglia. Irradiation causes double strand breaks and can lead to acute loss of microglia (Chen et al., 2016; Eriksson and Stigbrand, 2010; Kalm et al., 2009; Menzel et al., 2018; Xue et al., 2014). Surviving microglia can become activated, exhibiting an increase in expression of pro-inflammatory factors and reactive oxygen species and a change in morphology (Chen et al., 2016; Menzel et al., 2018; Monje et al., 2002; Moravan et al., 2011; Xue et al., 2014; Zhou et al., 2017). In mice, microglial activation has been reported within hours and as late as 6 months after cranial irradiation, demonstrating that irradiation has lasting effects (Chiang et al., 1993; Kyrkanides et al., 1999; Mildenberger et al., 1990; Mizumatsu et al., 2003; Moravan et al., 2011).

Other long-term effects of high dose cranial irradiation include reductions in microglial number (Han et al., 2016; Menzel et al., 2018), which may reflect an impaired ability of microglia to proliferate to replace other microglia that die throughout the lifespan (Askew et al., 2017). Indeed, some studies have shown that microglial proliferation is decreased acutely after irradiation (Chen et al., 2016; Han et al., 2016; Menzel et al., 2018), while others have shown increases in some brain areas (Hua et al., 2012; Monje et al., 2002). However, the long-term effects of irradiation on the capacity of microglia to proliferate are not well characterized.

Few studies have examined the effect of irradiation on microglial proliferation in response to CNS injury (Allen et al., 2014; Bosco et al., 2012; Gilmore et al., 2003). One report noted that irradiation reduced microglial proliferation in the context of spinal cord lesion, although these observations were not quantified (Gilmore et al., 2003). In a model of glaucoma, irradiated mice had fewer microglia proliferating in the optic nerve than unirradiated controls (Bosco et al., 2012). However, in both of these studies, animals were irradiated after injury; thus, decreases in the percentage of microglia positive for proliferation markers may be due to irradiation killing mitotic cells, and not a reflection of the ability of microglia to proliferate. Another study suggested that irradiation may exacerbate the effects of traumatic brain injury on microglial proliferation (Allen et al., 2014). Therefore, additional models in which irradiation is given prior to a proliferation-inducing stimulus may be informative.

The goal of this study was to determine if cranial irradiation has an acute and persistent effect on the ability of CNS-resident microglia to proliferate in response to brain injury. We used a sterile needle cortical stab model, which induces robust microglial proliferation (Amat et al., 1996; Zhu et al., 2003), to test the impact of irradiation given 1 week to 6 months prior to injury. We also investigated whether irradiation alters factors that are important for microglial injury detection and proliferation, such as P2Y12R, IL-34, CSF1 and CSF1R (Davalos et al., 2005; Gomez-Nicola et al., 2013; Haynes et al., 2006; Lou et al., 2016; Okubo et al., 2016; Raivich et al., 1998; Swiatkowski et al., 2016; Yamamoto et al., 2010, 2012). Lastly, we used a metastatic brain tumor model to investigate whether cranial irradiation prevents microglial proliferation in response to tumor growth.

2. Materials and methods

2.1. Animals

Subjects were 9- to 15-week-old male and female C57BL/6J mice obtained from Jackson Laboratories (Bar Harbor, ME). Male mice were used for the experiments presented in Figs. 1–6. Female mice were used for the experiment presented in Fig. 7. All animal procedures were reviewed and approved by the University of Rochester's Committee on Animal Resources and are fully compliant with the National Institute of Health guidelines. Mice were housed in groups of 3–5 animals per cage with free access to food and water, in temperature (23 °C ± 3 °C) and light (12:12 light:dark) controlled rooms. Cages of mice were assigned randomly to the experimental groups.

2.2. Irradiation

Mice were anesthetized with 100 mg/kg ketamine and 10 mg/kg xylazine administered by intraperitoneal (i.p.) injection and exposed to gamma radiation using a ^{137}Cesium source at the University of Rochester Medical Center (Rochester, NY). A lead collimator with a 5 mm slit was positioned to deliver radiation to the forebrain, while shielding the body, throat, esophagus, eyes and ears. Mice were positioned supine on the collimator. Doses of 1, 2.5, 5, 10 or 20 Gy were delivered at a rate of 1.25 Gy/min. Unirradiated control animals received anesthesia and were handled similarly to irradiated animals. Mice were returned to their home cages and returned to the vivarium after recovery from anesthesia.

2.3. Stab injury/sham surgeries

Animals received stab injury or sham surgery 1 w (Figs. 1–5) or 1 w, 1 m, 3 m, or 6 m after irradiation (Fig. 6) to test acute and long-term effects of irradiation. Animals were anesthetized with isoflurane (1.75% isoflurane in 30/70% oxygen/nitrogen) and secured on a stereotaxic apparatus (Kopf Instruments, Tunjunga, CA). Ophthalmic ointment was applied to the eyes and the hair over the scalp was cleared with Nair (Church and Dwight, Ewing, NJ). The scalp was sterilized with ethanol (70%) followed by iodine and was opened with a small incision made by a sterile scalpel. For both stab injury and sham surgery, a 0.5 mm burr hole was drilled 2.25 mm caudal and 1.5 mm lateral from bregma with a power drill. The hole was drilled to just above, but not through, the dura. For stab injury surgeries only, a 33 G (0.21 mm diameter) syringe needle (Hamilton, Reno, NV) was lowered slowly into the center of the hole over the course of 2 min to a depth of −1.1 mm from the surface of the brain. The needle was left in place for 2 min and then slowly retracted over the course of 2 min. Sham and stab injury burr holes were plugged with bone wax and the scalp incision was closed with veterinary adhesive. Post-surgery, animals received a single 0.3 mg/kg dose of buprenorphine subcutaneously and topical lidocaine to the scalp and were monitored for full recovery.

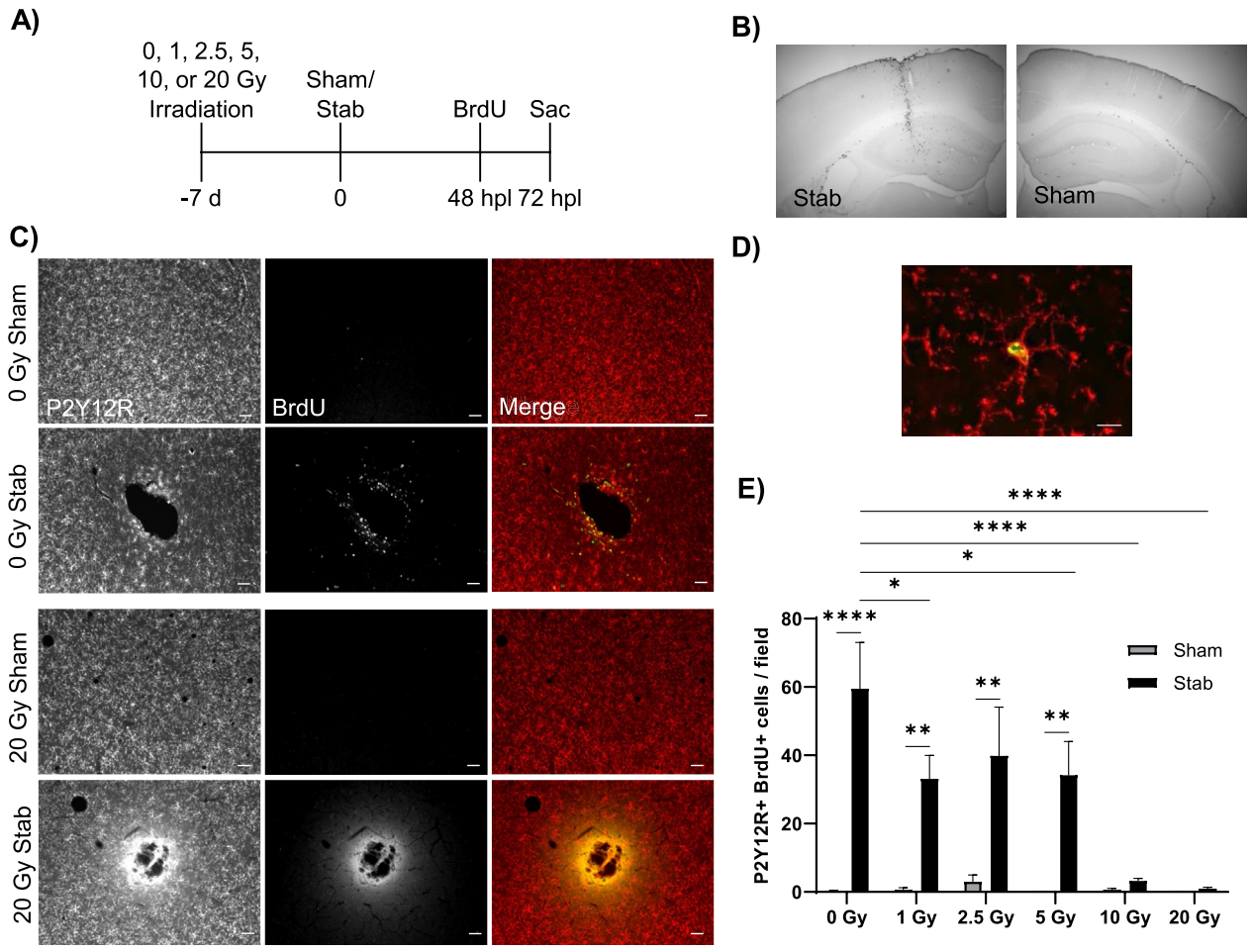

Fig. 1. Prior cranial irradiation prevents stab injury-induced microglial proliferation. A) Study design. Mice received cranial irradiation of 0, 1, 2.5, 5, 10, or 20 Gy. 1 w post-irradiation, mice received a cortical stab injury to one brain hemisphere and a sham surgery to the contralateral hemisphere. A single dose of BrdU was given 48 h post-lesion (hpl) and mice were sacrificed 72 hpl. **B)** Representative image of BrdU+ staining at the stab site in a coronal brain section. C**)** Representative P2Y12R and BrdU staining at stab injury or sham surgery sites, in 0 Gy control and 20 Gy irradiated mice. P2Y12R+ BrdU+ cells per image field were counted. Scale bars = 50 μm. **D)** Close up of a P2Y12R+ BrdU+ cell. Red = P2Y12R, green = BrdU. Scale bar = 10 μm. **E)** Quantification of P2Y12R+ BrdU+ cells per image field (897.43 × 667.85 μm), which was centered on the stab and sham surgery sites. N = 8 per group. Mean ± SEM shown. Two-way ANOVA with Sidak's correction for multiple comparisons. * indicates $p < 0.05$, **$p < 0.01$, ****$p < 0.0001$.

For the immunohistochemistry (IHC) studies, mice received a stab injury to one hemisphere and a sham surgery to the contralateral hemisphere. For the flow cytometry experiments, mice received two stab injuries, with the second stab injury 1.5 mm lateral and 1.0 rostral from bregma, and a second sham surgery at the corresponding coordinates on the contralateral hemisphere. After dissection (described below), tissue from both sham and both stab sites were combined for each animal to increase the total number of cells available for flow cytometry analysis. For the qRT-PCR experiments, mice received either two sham surgeries (one to each hemisphere) or two stab surgeries (one to each hemisphere), and tissues from the two surgical sites were pooled for each animal.

To ensure that irradiated and control mice received identical injuries, the same animal surgeon performed the surgeries on the same day, with the same equipment, following the same protocol for all mice. The order of surgery was randomized between irradiated and control mice and the technician was blinded to which group the mice belonged.

2.4. Tumor cell injection

For our metastatic brain tumor model, we used EO771 cells, which are derived from a spontaneously occurring mammary tumor in wild type C57BL/6J mice (Casey et al., 1951) and have been shown to metastasize to other tissues (Ewens et al., 2005; Johnstone et al., 2015). Cultured EO771 cells were a gift from Dr. Michelle Janelsins' Laboratory (University of Rochester Medical Center, Rochester, NY). Frozen cells were stored in liquid nitrogen until rapidly thawed in a 37 °C water bath. Cells were plated in sterile T-75 flasks with RPMI 1640 medium and incubated in an air chamber at 37 °C with 5% CO_2. Culture media was replaced with 10 ml fresh media after 4–8 h of incubation and replaced daily. On the day of injection, culture media was removed and the cells were rinsed with sterile 1X PBS. The cell layer was dispersed by adding 5 ml 0.05% Trypsin-EDTA and incubating for 2 min at 37 °C. 10 ml media was then added and cells were aspirated by gentle pipetting and centrifuged at 1000 rpm for 3 min. The supernatant was discarded and cells were washed in 10 ml HBSS three times. After the final wash, the cell pellet was resuspended in HBSS to a concentration of 10,000 cells per 1 μl and kept on ice until injection the same day.

Surgery was conducted similar to the stab wound surgery, described above. On the right hemisphere, 20,000 cells in 2 μl HBSS were injected into the striatum (0.5 mm rostral, 2.0 mm lateral, 2.5 mm ventral to bregma) at a rate of 0.2 μl per min, using a 30 G (0.31 mm diameter) syringe needle (Hamilton). After injection, the needle was left in place for 5 min and slowly retracted over the course of 2 min. Sham and injection site burr holes were plugged with bone wax and the scalp incision was closed with veterinary adhesive. Animals received a 0.3 mg/kg dose of buprenorphine subcutaneously and topical lidocaine to the scalp and

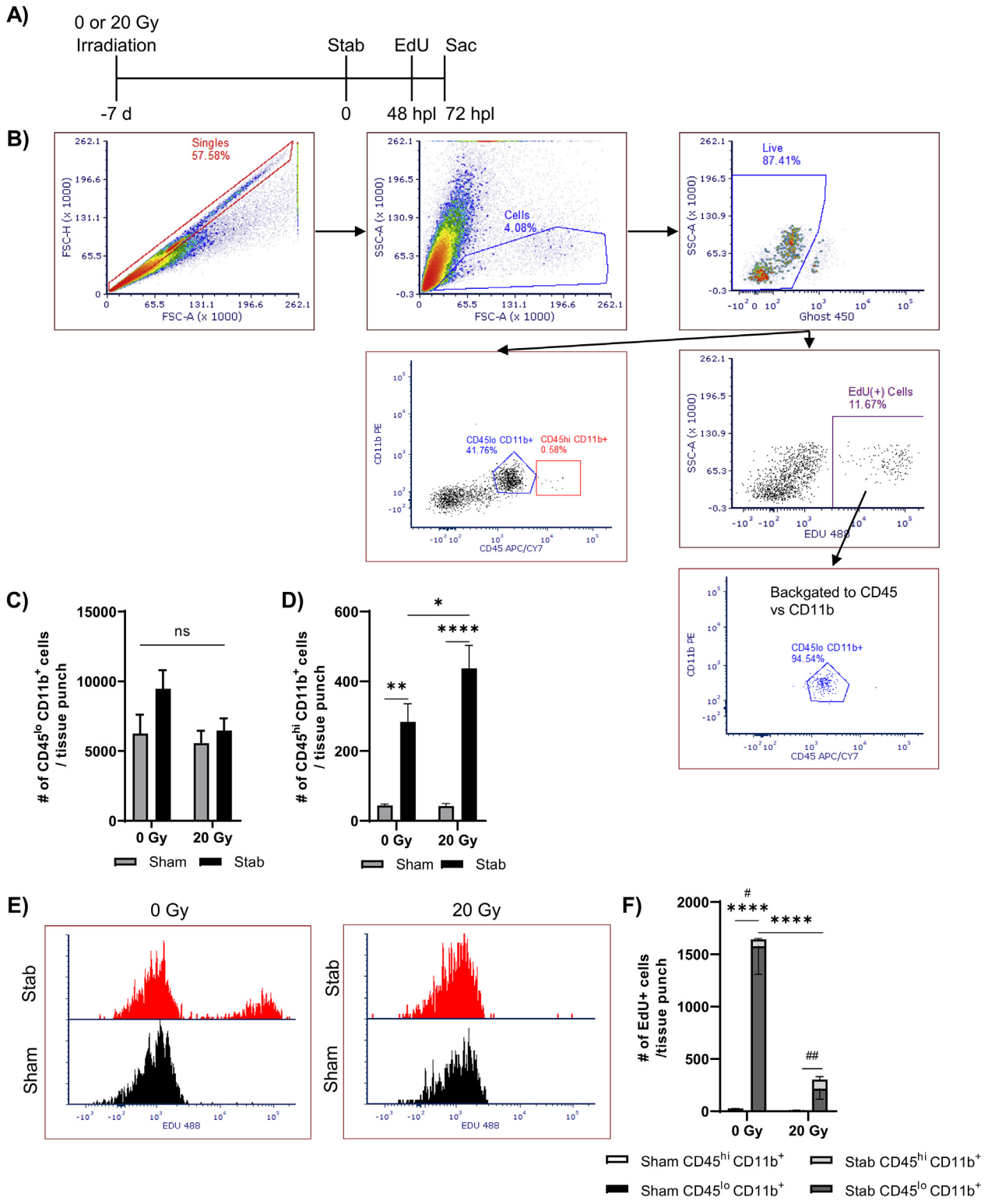

Fig. 2. Flow cytometry demonstrates that prior irradiation impairs stab-induced microglial proliferation and enhances recruitment of peripheral myeloid cells. A) Study design. Mice received 0 or 20 Gy cranial irradiation 1 w prior to receiving sham surgery on one brain hemisphere and stab surgery on the contralateral hemisphere. A single EdU injection was given 48 hpl and mice were sacrificed 72 hpl. **B)** Example of gating strategy used to exclude doublets, debris and dead cells, and to identify $CD45^{lo}$ $CD11b^{+}$ microglia, $CD45^{hi}$ $CD11b^{+}$ infiltrating myeloid cells, and EdU+ cells. Quantification of the number of cells in the **C)** $CD45^{lo}$ $CD11b^{+}$ and **D)** $CD45^{hi}$ $CD11b^{+}$ gates, regardless of EdU positivity, in a round punch of cortical tissue with a 3 mm diameter centered on each stab or sham injury site of irradiated and control mice. **E)** Representative histograms demonstrating EdU fluorescent intensity in $CD45^{lo}$ $CD11b^{+}$ cells from an unirradiated mouse and an irradiated mouse, which both received contralateral stab and sham surgeries. The lower fluorescing peak is the EdU negative population. **F)** Quantification of EdU+ cells that fall within the $CD45^{lo}$ $CD11b^{+}$ gate or $CD45^{hi}$ $CD11b^{+}$ gate. N = 6 per group. Mean ± SEM shown. Two-way ANOVA with Sidak's correction for multiple comparisons. *, #, indicate $p < 0.05$, ** and ##$p < 0.01$, ****$p < 0.0001$. Asterisks and hashtags refer to significant differences in $CD45^{lo}$ $CD11b^{+}$ and $CD45^{hi}$ $CD11b^{+}$ populations, respectively.

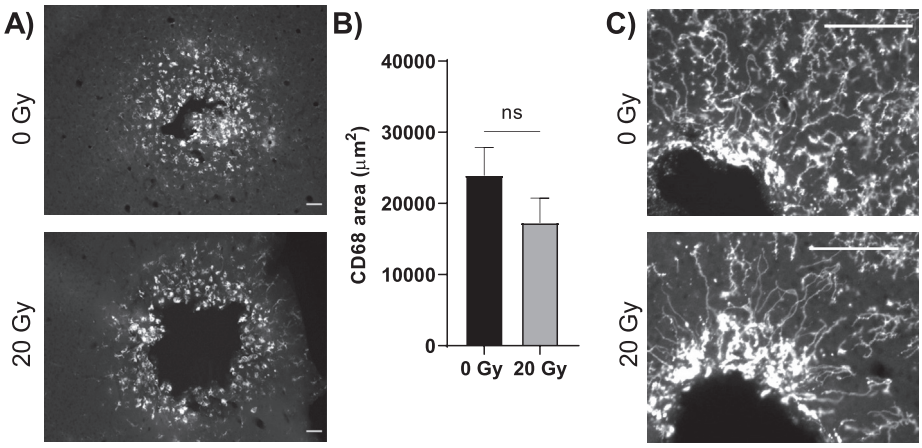

Fig. 3. Microglia in irradiated brains detect and respond to stab injury. A) Representative image of $CD68^+$ staining around the stab wound, 72 hpl, in 0 Gy control and 20 Gy irradiated mice. **B)** Quantification of CD68 positive area within a 10x image field (897.43 × 667.85 μm) centered on the stab wound, in 0 Gy and 20 Gy irradiated animals, 72 hpl. **C)** Representative images of P2Y12R+ microglial processes extending towards the stab wound 6 hpl in 0 Gy control and 20 Gy irradiated mice. N = 8 per group. Mean ± SEM shown. Unpaired student's t-test. * indicates $p < 0.05$. Scale bars = 50 μm.

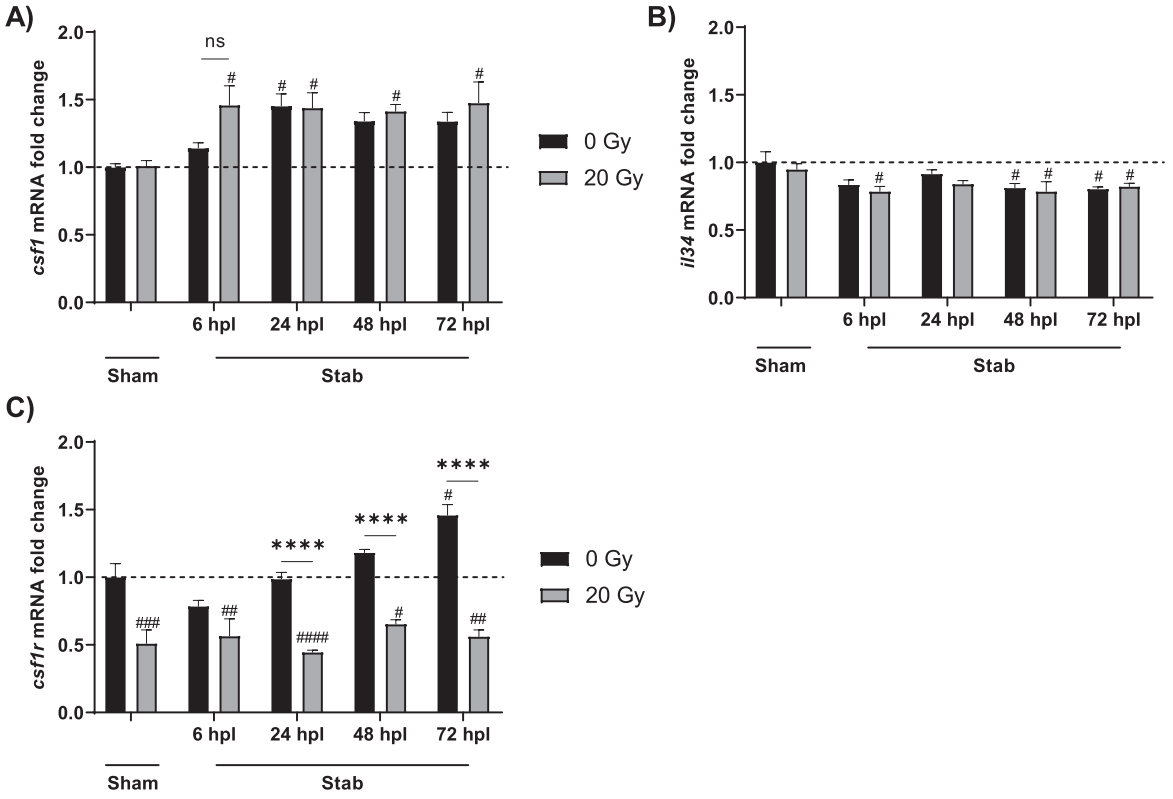

Fig. 4. mRNA levels for microglial proliferation-related genes change with stab injury and/or irradiation. Mice received 0 Gy or 20 Gy cranial irradiation 1 w prior to receiving sham or stab surgery. Stabbed mice were sacrificed 6, 24, 48, or 72 hpl. Sham mice were sacrificed at the time of the 6 hpl stab group. qRT-PCR for mRNA of **A)** *Csf1*, **B)** *Il34*, and **C)** *Csf1r*. N = 3–5 per group. Mean ± SEM shown. Two-way ANOVA with Sidak's correction for multiple comparisons. Every group was compared to the unirradiated sham group (significant differences indicated by hashtags). Additionally, 0 and 20 Gy groups were compared to each other, within each time point, to test the effect of irradiation. * and # indicates $p < 0.05$, ##$p < 0.01$, ***$p < 0.001$, **** and ####$p < 0.0001$.

were monitored for full recovery.

2.5. BrdU and EdU injections

Single injections of 150 mg/kg of Bromodeoxyuridine (BrdU, Sigma, St. Louis, MO) or 100 mg/kg of Ethynyldeoxyuridine (EdU, Carbosynth, San Diego, CA) dissolved in 0.9% NaCl were given i.p. at 2 or 24 h prior to sacrifice as described for each experimental paradigm. EdU was used for flow cytometry experiments in which the HCl treatment used for BrdU immunostaining was not compatible with co-labeling of other cellular antigens.

2.6. Tissue processing

Mice were deeply anesthetized with 540 mg/kg ketamine and 48 mg/kg xylazine delivered via i.p. injection. Mice were perfused transcardially with 0.15 M phosphate buffer (PB) with 0.5% w/v sodium nitrite and 2 IU/ml heparin.

For IHC analysis, mice were then perfused transcardially with approximately 50 ml ice-cold 4% paraformaldehyde in 0.15 M PB, pH 7.2. Dissected whole brains were immersion fixed for 2 additional hours at 4 °C before overnight immersion in 30% sucrose in 0.15 M PB. Whole brains were flash frozen in −78 °C isopentane and stored at −80 °C until

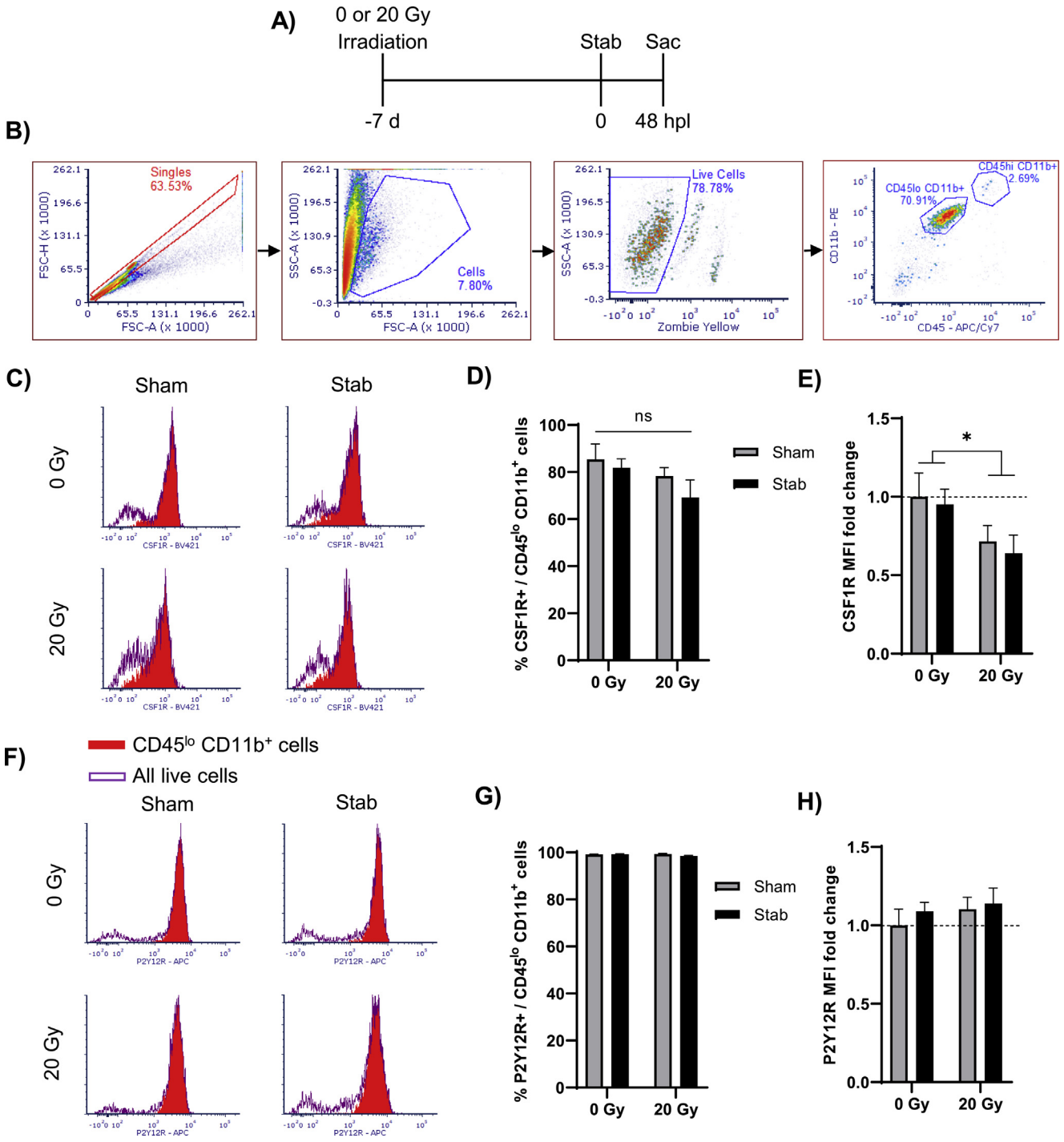

Fig. 5. Microglial CSF1R but not P2Y12R expression changes with irradiation. A) Study design. Mice were received 0 Gy or 20 Gy cranial irradiation 1 w prior to receiving two sham surgeries on one hemisphere and two stab surgeries on the contralateral hemisphere. Tissue from the two injury and two stab sites were pooled for flow cytometry. Mice were sacrificed 48 hpl. **B)** Example of gating strategy used to exclude doublets, debris and dead cells, and to identify $CD45^{lo}$ $CD11b^{+}$ microglia and $CD45^{hi}$ $CD11b^{+}$ infiltrating myeloid cells. **C)** Representative histograms of CSF1R median fluorescent intensity (MFI) in all live cells (purple) and in $CD45^{lo}$ $CD11b^{+}$ microglia (red) in each sham/stab and control/irradiated condition. **D)** Quantification of the percent of cells in the $CD45^{lo}$ $CD11b^{+}$ microglia gate that are positive for CSF1R. **E)** Quantification of the fold change of CSF1R MFI of $CD45^{lo}$ $CD11b^{+}$ microglia relative to the unstabbed unirradiated control. **F)** Representative histograms of P2Y12R median fluorescent intensity (MFI) in all live cells (purple) and in $CD45^{lo}$ $CD11b^{+}$ microglia (red) in each sham/stab and control/irradiated condition. **G)** Quantification of the percent of cells in the $CD45^{lo}$ $CD11b^{+}$ microglia gate that are positive for P2Y12R. **H)** Quantification of the fold change of P2Y12R MFI of $CD45^{lo}$ $CD11b^{+}$ microglia relative to the unstabbed unirradiated control. N = 6 per group. Mean ± SEM shown. Two-way ANOVA with Sidak's correction for multiple comparisons. * indicates main effect of irradiation, $p < 0.05$. (For interpretation of the references to colour in this figure legend, the reader is referred to the Web version of this article.)

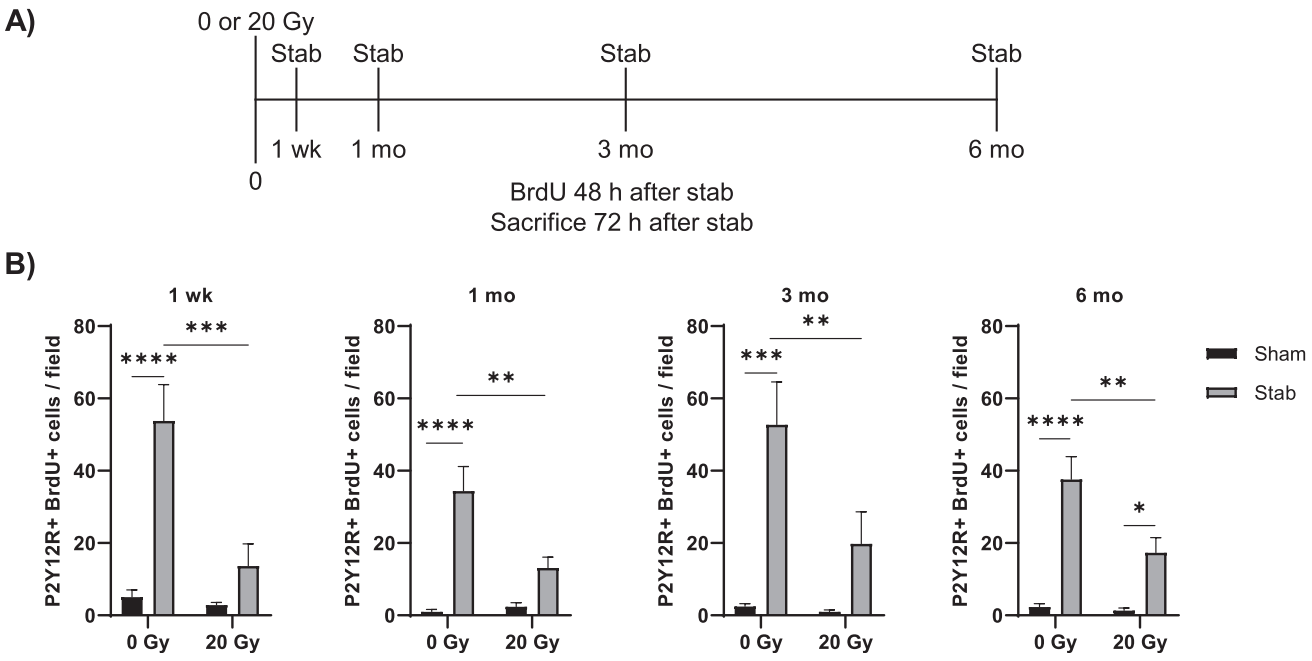

Fig. 6. Cranial irradiation leads to a long-term deficit in injury-induced microglial proliferation. A) Study design. Mice were exposed to 0 or 20 Gy cranial irradiation and subjected to stab on one hemisphere and sham surgery to the contralateral hemisphere at either 1 w, 1 m, 3 m, or 6 m after irradiation. Mice received a single BrdU injection 48 hpl and were sacrificed 72 hpl. **B)** Quantification of P2Y12R+ BrdU+ cells within a 10x image field (897.43 × 667.85 μm), centered on the stab and sham surgery sites, at each time point. N = 5–8 per group. Mean ± SEM shown. Two-way ANOVA with Sidak's correction for multiple comparisons. * indicates $p < 0.05$, ** $p < 0.01$, *** $p < 0.001$.

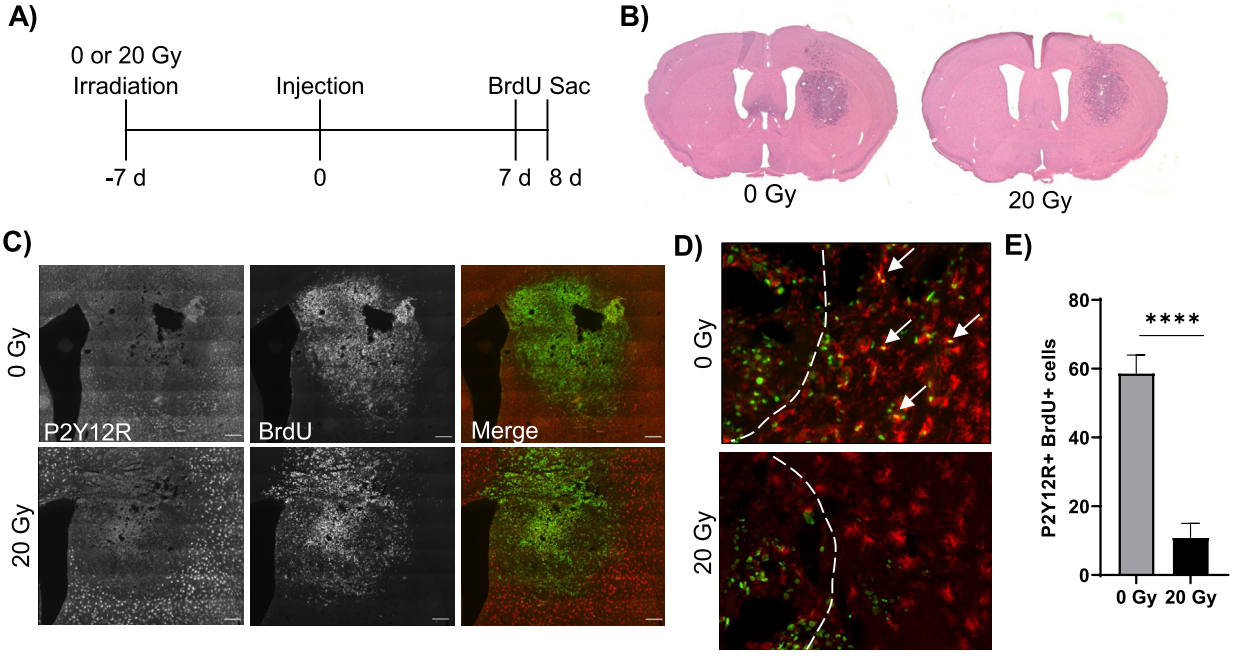

Fig. 7. Prior cranial irradiation reduces tumor-related microglial proliferation. A) Study design. Female mice were exposed to 0 or 20 Gy cranial irradiation 1 w prior to receiving a unilateral injection of EO771 breast adenocarcinoma cells to the striatum. 7 d post injection, mice received a single BrdU injection and were sacrificed 24 h later. **B)** Hemoxylin and eoxin staining of representative tissue sections. C) Representative images of P2Y12R and BrdU staining. Scale bars = 200 μm. **D)** Representative images of P2Y12R (red) and BrdU (green) staining around the tumor site. Arrows point to examples of double-positive cell staining. Dashed line indicates approximate tumor border. **E)** Quantification of P2Y12R+ BrdU+ cells. All P2Y12R+ BrdU+ cells on the hemisphere ipsilateral to the tumor were counted. N = 5–6 per group. Mean ± SEM shown. Unpaired student's t-test. **** indicates $p < 0.0001$. (For interpretation of the references to colour in this figure legend, the reader is referred to the Web version of this article.)

sectioning on a sliding microtome. For stab injury experiments, 25 μm horizontal sections were cut. For the tumor experiment, 30 μm coronal sections were cut. Free-floating sections were stored at −20 °C in cryoprotectant until processing for IHC.

For flow cytometry and qRT-PCR analysis, the cortex was dissected from the underlying brain tissue. Then a 3 mm round punch of cortex centered on each stab or sham surgery site was taken. For flow cytometry, tissue punches were immediately processed for analysis. For qRT-PCR, tissue was immediately flash frozen in isopentane and stored at −80 °C until processing.

2.7. Immunohistochemistry

Sections of brain tissue were washed in 0.15 M PB and blocked with 3% normal goat serum (GIBCO, Carlsbad, CA). For BrdU, antigen retrieval was performed by incubating free floating tissue sections in 4 N HCl for 20 min at room temperature. Staining of free-floating sections was performed using rabbit anti-P2Y12R (1:3000; Anaspec, Fremont, CA), rat anti-BrdU (1:300; Abcam, Cambridge, UK), and rat anti-CD68 (1:1000; Serotec, Raleigh, NC). Secondary antibodies included goat anti-rabbit Alexa 594 (1:2000; Invitrogen) and goat anti-rat Alexa 488 (1:2000; Invitrogen). To visualize BrdU for Fig. 1B, biotinylated goat anti-rat (1:1000; Vector, Burlingame, CA), followed by avidin-biotin complex kit solution (Elite Vectastain ABC, Vector) and subsequent 3-3' -diaminobenzidine reaction kits (Vector), were used according to the manufacturer's protocols. Hemoxylin and eoxin (H and E) were used to stain the tumor sections presented in Fig. 7B.

2.8. Image acquisition and analysis

A Zeiss Axioplan Ili light microscope (Zeiss, Germany) and Sensicam QE Camera (Cooke Optics, Mountain Lakes, NJ) were used to obtain all images. Slidebook software (Intelligent Imaging Innovations, Denver, CO) was utilized for image acquisition. ImageJ software (National Institutes of Health, Bethesda, MD) was used for analysis, as described. Slides were analyzed in a random order and in a blinded fashion.

Cell counting for BrdU and P2Y12R in the stab injury model: Cross hairs of the camera objective were centered on the stab wound or the corresponding area on the contralateral brain hemisphere and a 10x image was taken. Looking at the digital image of the BrdU channel only, the experimenter marked and counted all BrdU+ cells within the field of this 897.43 × 667.85 μm image, exclusive of edges, using the ImageJ Cell Counter plugin. Then, by looking through a 40x lens with a combined filter for detecting both Alexa Fluor 488 and 594 secondary antibodies, all previously counted BrdU+ cells were determined to be either P2Y12R+ or P2Y12R-, and were marked on the digital image in ImageJ. Counts from 2-3 sections per animal were averaged.

CD68 quantification in the stab injury model: For CD68 quantification, 10x images were acquired, centered on the stab wound, and thresholded in ImageJ to create a binary image where each pixel was deemed positive or negative for CD68. CD68 area measurement was calculated by converting total positive pixels per field to μm^2. 2-3 sections were averaged per animal.

Hole area quantification in the stab injury model: To quantify the area of the hole in the tissue made by the stab wound, 10x images were acquired, centered on the stab wound. ImageJ was used to trace the perimeter of the stab hole and calculate its area. 2-3 sections were averaged per animal.

Cell counting for BrdU and P2Y12R in the tumor model: All BrdU+ cells on the hemisphere of the brain ipsilateral to the tumor, excluding the tumor area (which contained few to no P2Y12R+ cells), were quantified and determined to be P2Y12R+ or P2Y12R-, as described above. The entire hemisphere ipsilateral to the tumor was quantified, since the tumor lesions were large. 2-3 sections per animal were averaged.

2.9. Flow cytometry

Tissue was dissociated into 0.5% BSA in 1x PBS (pH 7.2) buffer with a Dounce homogenizer (Cole-Parmer, Vernon Hills, IL), passed through a 70 μm strainer to create a single cell suspension, and centrifuged (7 min/240 G at 4 °C). Pelleted cells were incubated with myelin removal beads (Miltenyi, Bergisch Gladbach, Germany) and passed through an LS column attached to a MACS magnetic separator (Miltenyi) to remove myelin. After washing with PBS, cells were incubated with a fixable viability dye, Zombie Yellow (Biolegend) or Ghost Dye Violet 450 (Tonbo Biosciences, San Diego, CA) at room temperature. A Click-iT EdU Alexa Fluor 488 Flow Cytometry Assay Kit (Invitrogen) was used according to the manufacturer's instructions to label proliferating cells. Cells were then blocked with anti-CD16/32 Fc Block (2.4G2, BD Pharmingen, San Jose, CA) for 15 min at room temperature and stained for extracellular markers for 30 min at 4 °C. The following antibodies were used: anti-CD11b (M1/70), anti-CD45 (30-F11), anti-P2Y12R (S16007D) and anti-CSF1R (AFS98), all from Biolegend. CountBright counting beads (eBioscience, Fisher Scientific, Hampton, NH) were used to determine absolute numbers of cells in each sample, according to the manufacturer's protocol.

Samples were read with a LSRII cytometer (BD Biosciences, San Jose, CA). Gating and analysis was conducted in FCS Express 6 (De Novo Software, Glendale, CA). Side and forward scatter gating was used to exclude doublets and debris. Cellular internalization of viability stain was used to exclude dead cells. Fluorescent-minus-one and single-stained controls were used to determine positive antibody staining and/or EdU positivity among the live cells. CD11b and CD45 expression were used to identify $CD45^{lo}$ $CD11b^{+}$ microglia or $CD45^{hi}$ $CD11b^{+}$ infiltrating myeloid cells.

For calculation of CSF1R and P2Y12R fold change, median fluorescent intensities of CSF1R and P2Y12R were normalized to the respective medians of the unirradiated, unstabbed group.

2.10. qRT-PCR

Frozen tissue was homogenized and processed with an RNeasy Mini Kit (Qiagen, Hilden, Germany). RNA was quantified using a Nanodrop apparatus (Thermo Scientific, Waltham, MA) and 0.33 μg of total RNA was reverse transcribed with a Superscript III kit (Invitrogen). cDNA was stored at −20 °C until analysis with qRT-PCR. Reactions for *Csf1*, *Il34*, and *Csf1r* were performed as duplex reactions with *Gapdh* in a final volume of 10 μl with TaqMan Multiplex Master Mix and Taqman Kits (Applied Biosystems, Foster City, CA). Samples were denatured at 95 °C for 10 min, followed by 40 cycles of denaturing at 95 °C, annealing at 60 °C, and extension at 72 °C, each for 30 s. Samples were run in triplicate and threshold counts (Ct) averaged per sample. The efficiency of each reaction was determined using a dilution series of standards for each marker. To determine the fold increase of gene X relative to *Gapdh*, the following equation was used: $(1+\text{efficiency}^{GAPDH})^{Ct\ for\ GAPDH}/(1+\text{efficiency}^{X})^{Ct\ for\ X}$.

2.11. Statistical analyses

Sample size was determined by power analysis from preliminary data. For each analysis, data was collected in a random order and in a blinded fashion. Data was analyzed in Prism (GraphPad Software, version 8, San Diego, CA) using unpaired student's t-tests and one- and two-way analysis of variance (ANOVA). Sidak's correction for multiple comparisons was conducted where appropriate. All results are expressed as mean ±SEM. Subjects were deemed to be outliers at the time of data acquisition, before unblinding, if their tissue quality prevented accurate analysis. A p value < 0.05 was considered significant in all experiments.

3. Results

3.1. Prior cranial irradiation prevents stab injury-induced microglial proliferation

To test our hypothesis that cranial irradiation impairs the ability of microglia to proliferate, mice were exposed to 0, 1, 2.5, 5, 10 or 20 Gy cranial irradiation 1 w prior to receiving a unilateral stab injury (Fig. 1A). To assess irradiation effects that may be independent of stab, a sham surgery was conducted on the contralateral hemisphere of each animal (Fig. 1B). Mice received a single i.p. injection of BrdU to label proliferating cells 48 h post-lesion (hpl), a time at which stab-induced proliferation peaks (Fig S1). Mice were sacrificed 24 h after the BrdU injection (72 hpl) and IHC was performed to visualize P2Y12R and BrdU (Fig. 1C).

P2Y12R is a specific marker of microglia in the brain (Butovsky et al., 2014) and can be visualized with immunostaining to distinguish CNS-resident microglia from infiltrating macrophages. P2Y12R+ BrdU+ cells (Fig. 1D) were quantified to examine the effect of stab and irradiation on CNS-resident microglial proliferation (Fig. 1E). P2Y12R- BrdU+ cells were also quantified (Fig S2). Two-way ANOVA revealed a main effect of irradiation ($F(5, 72) = 5.311$, $p < 0.001$), stab ($F(1, 72) = 46.54$, $p < 0.0001$) and an interaction ($F(5, 72) = 5.131$, $p < 0.001$) on the number of P2Y12R+ BrdU+ cells per field (Fig. 1E). In unirradiated mice, the unstabbed hemisphere had few detectable P2Y12R+ BrdU+ cells (0.31 ± 0.19), confirming a low baseline turnover of microglia in the healthy cortex (Askew et al., 2017). No significant differences were seen between the unstabbed hemisphere of the unirradiated control group and the unstabbed hemispheres of any irradiated group, suggesting that at 1 w post irradiation, irradiation does not impact baseline microglial proliferation. In unirradiated animals, stab injury significantly increased the P2Y12R+ BrdU+ cell count per field (59.6 ± 13.5). While stab injury did cause a significant increase in P2Y12R+ BrdU+ cells in 1, 2.5, and 5 Gy animals, these stab-induced increases were blunted compared to that of controls (1 Gy: 33.1 ± 6.8, $p < 0.05$; 2.5 Gy: 40.0 ± 14.1, $p = 0.17$; 5 Gy: 34.2 ± 9.8, $p < 0.05$). The effect of 10 and 20 Gy irradiation was so profound that stab injury failed to increase P2Y12R+ BrdU+ cells in these animals. These data indicate that the ability of microglia to proliferate in response to stab injury is acutely impaired by prior cranial irradiation in a dose-dependent manner.

3.2. Flow cytometry demonstrates that prior irradiation impairs stab-induced microglial proliferation and enhances recruitment of peripheral myeloid cells

We next sought to determine whether stab injury and/or irradiation altered the overall number of microglia and whether these insults impacted the infiltration of myeloid cells from peripheral circulation into the brain. We additionally sought to quantify the relative contribution of CNS-resident microglia versus infiltrating myeloid cells to the proliferation response in our model. Mice were given stab and sham surgeries 1 w after 0 or 20 Gy irradiation. EdU was injected 48 hpl, mice were sacrificed at 72 hpl, and tissue was immediately processed for flow cytometry (Fig. 2A). Cells were gated according to CD45, CD11b, and EdU expression (Fig. 2B) and counting beads were used to calculate cell numbers in a round punch of cortical tissue with a 3 mm diameter centered on the stab or sham injury site.

First, we quantified the overall number of $CD45^{lo}$ $CD11b^{+}$ (Fig. 2C) and $CD45^{hi}$ $CD11b^{+}$ cells (Fig. 2D), regardless of EdU expression, in tissue of each stabbed and unstabbed, irradiated and unirradiated condition. Neither stab injury nor irradiation impacted the number of $CD45^{lo}$ $CD11b^{+}$ cells; however, there was a trend towards increased numbers in the unirradiated stabbed animals ($p = 0.11$), which may reflect increased microglial proliferation and subsequent increases in microglial number following stab alone. In contrast, stab injury increased the count of $CD45^{hi}$ $CD11b^{+}$ cells in the brains of both unirradiated and irradiated mice ($p < 0.01$ and $p < 0.0001$), suggesting that peripheral myeloid cells infiltrate the brain in response to needle stab injury. Interestingly, while irradiation alone did not increase the $CD45^{hi}$ $CD11b^{+}$ cell number, it heightened the stab response, leading to more $CD45^{hi}$ $CD11b^{+}$ cells than in the unirradiated stabbed brain ($p < 0.05$). One interpretation of these data is that irradiation led to a preconditioned state that enhanced monocyte infiltration when the brain was subsequently injured (Moravan et al., 2016). Alternatively, peripheral monocytes may have infiltrated to compensate for the diminished resident microglial response (Fig. 2F) (Varvel et al., 2012).

Next, to analyze proliferation in response to stab injury, EdU+ positive cells were identified as being $CD45^{lo}$ $CD11b^{+}$ microglia or $CD45^{hi}$ $CD11b^{+}$ infiltrating myeloid cells and quantified (Fig. 2E and 2F). In both unirradiated and irradiated mice, few EdU+ cells were seen in the sham surgery condition, indicating that baseline proliferation rates are low. In unirradiated animals, stab injury significantly increased the number of EdU+ cells ($p < 0.0001$); these cells were mostly comprised of $CD45^{lo}$ $CD11b^{+}$ cells (86.2 ± 7.1%), with some $CD45^{hi}$ $CD11b^{+}$ cells (4.1 ± 2.5%), suggesting that the majority of proliferating cells isolated from the tissue punches were CNS-resident microglia and not infiltrating myeloid cells. Similar to our results assessing P2Y12R+ and BrdU+ by IHC, 20 Gy cranial irradiation drastically reduced the number of $CD45^{lo}$ $CD11b^{+}$ microglia that were EdU+ in stabbed tissue ($p < 0.0001$), such that the number of EdU+ microglia was not different in the irradiated sham versus irradiated stabbed condition ($p = 0.46$). These data support our IHC experiments (Fig. 1) which showed low baseline microglial proliferation in the uninjured brain, a robust upregulation of CNS-resident microglial proliferation following stab injury, but an impaired stab-induced proliferation response in previously irradiated animals. The number of EdU+ $CD45^{hi}$ $CD11b^{+}$ cells in the stabbed cortex did not decline with cranial irradiation, possibly because these cells proliferated in and emerged from the bone marrow after irradiation, as would be expected with their short lifespan (van Furth and Cohn, 1968; Yona et al., 2013).

3.3. Microglia in irradiated brains detect and respond to stab injury

Our IHC and flow cytometry data demonstrated that prior high dose cranial irradiation significantly reduced stab-induced microglial proliferation (Figs. 1E and 2F). We next investigated whether microglia in irradiated mice were still able to detect and respond in other ways to stab injury. 0 and 20 Gy tissues, generated for the experiment presented in Fig. 1, were stained for CD68, a marker associated with monocyte activation and phagocytosis, which has been shown to be upregulated in response to brain injury (Fu et al., 2014). CD68 was upregulated around the stab site in the brains of both irradiated and unirradiated mice (Fig. 3A). An unpaired student's t-test demonstrated no significant differences in $CD68^{+}$ area per field around the stab wound in unirradiated and irradiated mice ($t = 1.276$, $df = 14$, $p = 0.228$, Fig. 3B), suggesting that microglia in mice exposed to high dose cranial irradiation retained functionality with respect to their ability to upregulate CD68 in response to injury. There was a significant decrease in the area of the hole left in the tissue from stab wound (unirradiated: 31,937 ± 3643 μm^2, irradiated: 17,134 ± 3719 μm^2, mean ± SEM), which may reflect an altered ability of microglia or other cells in the irradiated brain to clear damaged tissue from the wound site.

In the injured brain, microglia are known to extend their processes towards the lesion site (Davalos et al., 2005; Lou et al., 2016; Swiatkowski et al., 2016). In our tissues, we observed that microglia in the brains of irradiated mice demonstrated comparable P2Y12R+ process extension towards the lesion to the unirradiated mice (Fig. 3C), suggesting that cranial irradiation does not prevent microglial injury detection or process extension. Therefore, post-irradiation deficits in microglial proliferation are not likely due to the inability of microglia to detect injury.

3.4. mRNA levels for microglial proliferation-related genes change with stab injury and/or irradiation

CSF1 and IL-34 are cytokines that bind the CSF1R on microglia and are important regulators of microglial proliferation under homeostatic conditions. Additionally, CSF1 has been shown to increase and induce microglial proliferation in many models of CNS injury (Guan et al., 2016; Okubo et al., 2016; Raivich et al., 1998; Takeuchi et al., 2001; Yamamoto et al., 2010, 2012). Injury and increases in CSF1 can lead to CSF1R upregulation, which potentially serves to increase microglial sensitivity to CSF1 (Okubo et al., 2016; Raivich et al., 1998). We sought to quantify potential changes in CSF1, IL-34 and CSF1R in our stab model and determine whether cranial irradiation altered the stab response. Mice were exposed to 0 or 20 Gy cranial irradiation 1 w prior to receiving sham or stab surgery and sacrificed 6, 24, 48, or 72 hpl. mRNA for *Csf1*, *Il34* and C*s1r* in 3 mm diameter round tissue punches centered around the stab and sham surgery sites were quantified by qRT-PCR.

Csf1 mRNA levels increased in response to stab injury in both 0 Gy controls and 20 Gy irradiated mice (two-way ANOVA, main effect of time after stab ($F(4, 37 = 5.667)$, $p < 0.01$), Fig. 4A), and there were no significant differences between unirradiated and irradiated mice at any post-stab/sham time point, although there was a trend at 6 hpl ($p = 0.09$). Stab injury significantly elevated *Csf1* mRNA at 24 hpl in unirradiated mice ($p < 0.05$), and there was a trend towards increased *Csf1* at 48 and 72 hpl ($p = 0.11$, for both). In irradiated mice, stab injury increased *Csf1* mRNA at all time points post-injury, relative to the unstabbed unirradiated tissue ($p < 0.05$).

Il34 mRNA levels decreased in response to stab injury in both 0 Gy controls and 20 Gy irradiated mice (two-way ANOVA, main effect of time after stab ($F(4, 37) = 5.678$, $p < 0.01$), Fig. 4B), and there were no significant differences between unirradiated and irradiated mice at any post-stab/sham time point. In unirradiated mice, stab injury significantly reduced *Il34* mRNA at 48 and 72 hpl ($p < 0.05$). In irradiated mice, *Il34* mRNA was significantly reduced 6, 48, and 72 hpl ($p < 0.05$), relative to the unstabbed unirradiated tissue.

Interestingly, *Csf1r* was differentially affected in 0 Gy controls versus 20 Gy irradiated mice (two-way ANOVA, main effect of stab: ($F(4, 37) = 9.425$, $p < 0.0001$), irradiation: ($F(1, 37) = 154.2$, $p < 0.0001$), interaction: ($F(4, 37) = 6.818$, $p < 0.001$)), (Fig. 4C). In unirradiated controls, stab injury increased *Csf1r* mRNA significantly at 72 hpl ($p < 0.05$). In contrast, irradiation alone significantly reduced *Csf1r* mRNA ($p < 0.05$) and low *Csf1r* levels persisted, not rising at any time measured after stab injury.

3.5. Microglial CSF1R but not P2Y12R expression changes with irradiation

To determine whether the effect of irradiation on *Csf1r* extends to protein expression and to specify it to microglia, we analyzed microglial CSF1R protein expression by flow cytometry. A new set of mice were exposed to 0 or 20 Gy 1 w prior to sham or stab surgery and sacrificed 48 hpl (Fig. 5A), at the determined peak of microglial proliferation (Fig S1), when CSF1R-mediated signaling is likely to be important. Cells were gated according to CD45 and CD11b expression (Fig. 5B).

First, we verified that CSF1R expression was confined to $CD45^{lo}$ $CD11b^{+}$ microglia in tissue from all four unstabbed/stabbed and unirradiated/irradiated conditions (Fig. 5C). Next, we analyzed whether the percent of $CD45^{lo}$ $CD11b^{+}$ microglia that were positive for CSF1R was altered by stab and/or irradiation (Fig. 5D). Two-way ANOVA revealed no differences between any of the conditions, demonstrating no effect of stab ($F(1, 20) = 1.251$, $p = 0.28$) or irradiation ($F(1, 20) = 1.251$, $p = 0.09$), and no interaction ($F(1, 20) = 0.25$, $p = 0.62$). Having determined that the percent of total microglia that were positive for CSF1R did not change, we next investigated whether the level of CSF1R expression decreased on $CD45^{lo}$ $CD11b^{+}$ microglia in any of our conditions (Fig. 5E). Irradiation reduced median fluorescent intensity of CSF1R on microglia (two-way ANOVA ($F(1, 20) = 6.35$, $p < 0.05$), but we did not detect an effect of stab. These data confirm our qRT-PCR data, which demonstrated that at 48 hpl, stab injury does not yet significantly increase CSF1R expression in unirradiated mice (Fig. 4C), and that irradiation decreases CSF1R expression.

Some studies have shown that microglial P2Y12R expression also changes in the context of injury and inflammation (Haynes et al., 2006). We investigated whether irradiation and/or stab injury altered P2Y12R expression in our model. First, we confirmed that P2Y12R expression was confined to $CD45^{lo}$ $CD11b^{+}$ microglia (Fig. 5F). Next, we quantified the percent of $CD45^{lo}$ $CD11b^{+}$ microglia that expressed P2Y12R and detected no changes with irradiation and/or stab (Fig. 5G). Lastly, median fluorescent intensity of P2Y12R was quantified in $CD45^{lo}$ $CD11b^{+}$ microglia (Fig. 5H). There were no significant differences in P2Y12R expression with irradiation, stab, or both, demonstrating that neither stab injury nor irradiation affected microglial P2Y12R expression, at the time point analyzed.

3.6. Cranial irradiation leads to a long-term deficit in injury-induced microglial proliferation

Cranial irradiation has been shown to lead to a long-term impairment in the proliferation of some cell populations in the brain, including OPCs and NPCs (Begolly et al., 2018; Mizumatsu et al., 2003; Sweet et al., 2014, 2016). We hypothesized that cranial irradiation would have a long-lasting impact on the ability of microglia to proliferate in response to stab injury, relative to unirradiated controls. To test this, mice were exposed to 0 or 20 Gy cranial irradiation, as previously described, but then subjected to contralateral stab and sham surgeries at a range of intervals, 1 w, 1 m, 3 m, or 6 m after irradiation (Fig. 6A). Mice at each time point received a single i.p. BrdU injection 48 hpl and were sacrificed 72 hpl.

P2Y12R+ BrdU+ cells were quantified around the sham surgery and stab injury sites in unirradiated and irradiated mice at each time point (Fig. 6B). At all time points, there were few P2Y12R+ BrdU+ cells in the sham surgery tissue, with no significant differences between irradiated and unirradiated groups. At each time point, stab significantly increased P2Y12R+ BrdU+ cells per field in unirradiated animals, demonstrating that CNS-resident microglia proliferate in response to injury, even in older mice. Importantly, at every time point, animals that had been previously irradiated had fewer P2Y12R+ BrdU+ cells around the stab injury site, relative to unirradiated controls, suggesting that cranial irradiation impairs injury-induced microglial proliferation, even when the injury occurs long after irradiation.

3.7. Prior cranial irradiation reduces tumor-related microglial proliferation

Because cranial irradiation is a component of cancer therapy for many patients, we sought to examine the proliferation of microglia in response to tumor growth and determine if prior irradiation impairs this proliferation response. Mice were exposed to 0 or 20 Gy cranial irradiation 1 w prior to receiving 20,000 EO771 cells injected directly into the striatum. 1 w post injection, mice received a single i.p. dose of BrdU and were sacrificed 24 h later (Fig. 7A). This interval allowed the microglial proliferation related to the needle insertion to abate (Buffo et al., 2005) and the tumor to establish and grow (Fig. 7B).

Tissue sections were stained for P2Y12R and BrdU (Fig. 7C). The lesions consistently included large numbers of BrdU+ cells, demonstrating that the tumor was highly proliferative, regardless of the radiation condition. However, while P2Y12R+ cells were present throughout the brain and in the periphery of the tumor, the lesions were mostly devoid of P2Y12R+ cells, suggesting that P2Y12R+ microglia may not infiltrate the tumor used in this model. Importantly, cells that were positive for both P2Y12R and BrdU surrounded the tumor in unirradiated controls (Fig. 7D), whereas prior cranial irradiation led to a significant reduction in P2Y12R+ BrdU+ cell numbers ($t = 7.126$, $df = 8$, $p < 0.001$, Fig. 7E).

This suggests that prior cranial irradiation altered the proliferative response of microglia to brain tumor growth.

4. Discussion

Because patients with cancer are now living longer, it is becoming increasingly important to consider the long-term side effects of cancer treatment, including the effects of irradiation on the brain (DeSantis et al., 2014). Microglia, the tissue resident macrophage of the CNS, play many important roles in maintaining brain homeostasis. Microglial proliferation is a component of the CNS response to many brain insults, including stroke, traumatic brain injury, tumor growth, Aβ deposition and neurodegeneration; in some injuries, this proliferative response may be important for brain repair (Ahn et al., 2018; Gomez-Nicola et al., 2013; Kamphuis et al., 2012; Li et al., 2013; Olmos-Alonso et al., 2016). Given the anti-proliferative effects that irradiation has on other cell types, cranial irradiation may impact how microglia proliferate in response to CNS injuries. However, data demonstrating the effect of prior cranial irradiation on injury-induced microglial proliferation is limited (Allen et al., 2014).

The goal of this study was to determine whether prior cranial irradiation impairs the ability of CNS-resident microglia to proliferate in response to injury or tumor growth. We demonstrated that exposure to 1 and 5 Gy cranial irradiation reduced, and 10 and 20 Gy abolished, the microglial proliferation response to subsequent stab injury, in mice. Additionally, we showed that a 20 Gy dose reduced microglial proliferation in response to a stab injury that was given 6 months after irradiation. These data suggest that the effect of irradiation on microglial proliferation is long-lasting. Given the role of microglial proliferation in the context of many brain injuries and diseases, a long-term reduction in microglial proliferation after cranial radiotherapy may leave patients' brains more vulnerable to the effects of future morbidities. However, we note that most of the experiments reported herein used a higher dose of radiation than typically given to patients in the clinic. This may limit the clinical relevance of the data we show, which will need to be followed up with studies at lower doses.

Our data may also have implications for patients who receive cranial radiotherapy prior to CNS tumor resection (Udovicich et al., 2019) or for prophylactic purposes to prevent the spread of high-risk disease to the CNS (Jeha et al., 2019; Manapov et al., 2018; Slotman et al., 2007; Yin et al., 2019). While cranial irradiation is often given after tumor resection, it has been proposed that stereotactic irradiation be given before surgical removal of a brain tumor in an effort to reduce leptomeningeal disease (Udovicich et al., 2019). Since microglial proliferation is important for wound healing and combatting infection (Bellver-Landete et al., 2019; Chen et al., 2019; Lalancette-Hebert et al., 2007; Rice et al., 2017), our data suggest that potential for alterations in the proliferative capacity of microglia after irradiation may impact healing or contribute to post-surgical complications. Indeed, we saw that prior irradiation decreased the area of the hole left in the cortical tissue due to the stab wound, which may reflect an altered ability of microglia to phagocytose damaged tissue from the wound site. Additional experiments are necessary to determine whether and to what extent microglial phagocytic capacity is altered by irradiation. Our data also suggest that prior irradiation may impact how microglia respond to new tumor growth in patients with metastatic disease.

We utilized a brain tumor metastasis model to continue our investigation of the impact of irradiation on the microglial proliferation response. Overall, our data showed that CNS-resident microglial proliferation was increased in the periphery of a tumor, but that this response was blunted by prior cranial irradiation. The role of microglia and microglial proliferation in the context of brain tumors is complex, since microglia can assume either an anti-tumorigenic or pro-tumorigenic role (Roesch et al., 2018). Since it is unclear as to the conditions that determine whether newly proliferated microglia adopt a pro-tumor or anti-tumor phenotype, further studies are necessary to determine whether an irradiation-related reduction in the microglial proliferation response is beneficial or detrimental to the host, in the context of a tumor. For example, if microglia in the tumor border are resisting tumor growth, fewer microglia, as a result of impaired proliferation, could result in faster and more diffuse tumor expansion into the surrounding tissue. Whether irradiation impacts the microglial-tumor cell relationship is an interesting question, although beyond the scope of this present work.

Historically, radiation biologists proposed that the radiation effects seen in normal tissues were the result of cell killing and were directly correlated with DNA damage. However, more recently, consideration has been given to the understanding that cells and tissues respond to irradiation in complex ways and that many factors contribute to irradiation-induced cell death (Prise et al., 2005; Williams et al., 2016). Likewise, irradiation impacts cell proliferation in a complex way (Di Maggio et al., 2015), and the effects may be tissue dependent. We investigated how irradiation may impact brain injury detection and microglial proliferation by examining the effect of irradiation on P2Y12R, CSF1, IL-34 and CSF1R, critical factors in the brain's normal response to injury.

When the brain is injured, soluble factors, such as ATP, are released from damaged cells and subsequently bind to receptors on microglia, such as P2Y12R, leading to microglial process extension toward the injury site, microglial translocation through tissue, and blood brain barrier repair (Davalos et al., 2005; Eyo et al., 2018; Lou et al., 2016; Swiatkowski et al., 2016). In our experiment, microglia in both irradiated and unirradiated mice extended their processes towards the injury site, demonstrating their ability to detect the wound. Additionally, our data show that irradiation did not affect P2Y12R expression on microglia, in contrast to another model of microglial activation (Haynes et al., 2006). These findings are important for the interpretation of our IHC quantification of microglial proliferation in response to stab injury, since P2Y12R was used as a marker to quantify CNS-resident microglia. Our study also demonstrated that microglia in irradiated brains maintain their ability to respond in other ways to brain injury, such as increasing the activation and phagocytic marker, CD68. These data demonstrate that not all functions of microglial injury response are lost in animals exposed to high-dose irradiation, despite a demonstrated loss of proliferative capacity.

CSF1 and IL-34 both bind to the CSF1R and stimulate microglial proliferation under homeostatic conditions, although CSF1 may be more important for injury responses (Ginhoux et al., 2010; Lin et al., 2008; Okubo et al., 2016; Wang and Colonna, 2014). Indeed, in the context of injury, CSF1 is released by damaged cells and stimulates microglial proliferation, while IL-34 expression decreases, is unaltered, or increases only temporarily (Chihara et al., 2010; Gomez-Nicola et al., 2013; Greter et al., 2012; Okubo et al., 2016; Yamamoto et al., 2010). We demonstrated that levels of mRNA for *Csf1* increased while *Il34* levels decreased in response to needle stab injury, confirming prior studies demonstrating a difference between *Csf1* and *Il34* injury responses. Additionally, since these responses were unaffected by irradiation, it appears unlikely that the impairment in injury-induced microglial proliferation seen in the irradiated mice was due to alterations in the ability of injured tissue to express *Csf1* or *Il34*.

Microglia are the main cell type that expresses CSF1R in the brain (Zhang et al., 2014) and CSF1R-mediated signaling is critical for microglial proliferation and survival. Indeed, pharmacological blockade or genetic knockout of CSF1R leads to a loss of microglia and their ability to maintain baseline proliferation (Elmore et al., 2014; Erblich et al., 2011; Greter et al., 2012; Oosterhof et al., 2018). Additionally, reducing CSF1R-mediated signaling has been shown to dampen injury-induced microglial proliferation (Berezovskaya et al., 1995; Okubo et al., 2016; Raivich et al., 1994); however, to our knowledge, the effect of irradiation on microglial CSF1R has not been previously studied. Our data demonstrated that irradiation reduced *Csf1r* mRNA levels in cortical tissue and reduced CSF1R protein expression on microglia. These data provide evidence that reductions in CSF1R expression after cranial irradiation may decrease microglial sensitivity to the proliferative signal of CSF1, and

thereby contribute to a blunted proliferation response of microglia to injury. Interestingly, *Csf1r* mRNA levels increased after injury in unirradiated controls, consistent with other studies (Yamamoto et al., 2010, 2012); however, *Csf1* levels were persistently decreased in irradiated mice, not increasing in response to stab. Follow up studies could investigate how irradiation impacts regulators of CSF1R expression, such as the C/EBPα-PU.1 pathway (Bonifer and Hume, 2008; Celada et al., 1996; Zhang et al., 1999), to elucidate possible mechanisms of impaired microglial CSF1R upregulation in response to injury in irradiated animals.

Because CSF1R is expressed on microglia, changes in the level of *Csf1r* mRNA measured in tissue samples could reflect changes in the overall number of microglia. However, our flow cytometry experiment provided evidence that microglial number was unchanged after irradiation at the acute time points analyzed. Furthermore, flow cytometry demonstrated that the amount of CSF1R expressed on microglia was decreased after irradiation. CSF1R quantification was not affected by microglial number using this method, since fluorescent intensity for the CSF1R antibody was quantified for individual microglial cells. Therefore, we interpret our data as a reflection of a true reduction in CSF1R expression on microglia after irradiation, and not a result of there being fewer microglia present in the tissue samples.

In summary, we confirmed our hypothesis that cranial irradiation reduces microglial proliferation in response to a needle stab injury and that this impairment is long-lasting. We demonstrated that irradiated microglia can detect a stab injury, but that reduced CSF1R expression may contribute to impaired injury-induced microglial proliferation in irradiated mice. Lastly, we demonstrated that prior cranial irradiation impairs the proliferation response of microglia to the growth of a tumor. Because of the important role of microglial proliferation in maintaining brain homeostasis and contributing to brain repair, and the intersection of irradiation and brain trauma in patients with cancer, continued investigation of irradiation-induced changes in microglial proliferation is important for understanding the effects of cranial irradiation on cancer survivors and for potentially developing strategies to mitigate side effects of cranial radiotherapy.

Funding

This work was supported by research grants from the National Institute of Allergy and Infectious Diseases (U19AI091036) and NASA (NNX16AE07G). EB received support from the National Institute of Neurological Disorders and Stroke F31NS101750 and the National Cancer Institute T32CA102618.

Declaration of competing interest

None.

Acknowledgements

We thank Lee Trojanczyk and Valerie Grose for their technical assistance with animal handling and tissue processing. We thank Bryan Thompson for culturing the EO771 cells.

Appendix A. Supplementary data

Supplementary data to this article can be found online at https://doi.org/10.1016/j.bbih.2020.100057.

References

Ahn, S.J., Anrather, J., Nishimura, N., Schaffer, C.B., 2018. Diverse inflammatory response after cerebral microbleeds includes coordinated microglial migration and proliferation. Stroke 49, 1719–1726.

Ajami, B., Bennett, J.L., Krieger, C., Tetzlaff, W., Rossi, F.M., 2007. Local self-renewal can sustain CNS microglia maintenance and function throughout adult life. Nat. Neurosci. 10, 1538–1543.

Allen, A.R., Eilertson, K., Chakraborti, A., Sharma, S., Baure, J., Habdank-Kolaczkowski, J., Allen, B., Rosi, S., Raber, J., Fike, J.R., 2014. Radiation exposure prior to traumatic brain injury induces responses that differ as a function of animal age. Int. J. Radiat. Biol. 90, 214–223.

Amat, J.A., Ishiguro, H., Nakamura, K., Norton, W.T., 1996. Phenotypic diversity and kinetics of proliferating microglia and astrocytes following cortical stab wounds. Glia 16, 368–382.

Askew, K., Li, K., Olmos-Alonso, A., Garcia-Moreno, F., Liang, Y., Richardson, P., Tipton, T., Chapman, M.A., Riecken, K., Beccari, S., Sierra, A., Molnar, Z., Cragg, M.S., Garaschuk, O., Perry, V.H., Gomez-Nicola, D., 2017. Coupled proliferation and apoptosis maintain the rapid turnover of microglia in the adult brain. Cell Rep. 18, 391–405.

Begolly, S., Olschowka, J.A., Love, T., Williams, J.P., O'Banion, M.K., 2018. Fractionation enhances acute oligodendrocyte progenitor cell radiation sensitivity and leads to long term depletion. Glia 66, 846–861.

Bellver-Landete, V., Bretheau, F., Mailhot, B., Vallieres, N., Lessard, M., Janelle, M.E., Vernoux, N., Tremblay, M.E., Fuehrmann, T., Shoichet, M.S., Lacroix, S., 2019. Microglia are an essential component of the neuroprotective scar that forms after spinal cord injury. Nat. Commun. 10, 518.

Berezovskaya, O., Maysinger, D., Fedoroff, S., 1995. The hematopoietic cytokine, colony-stimulating factor 1, is also a growth factor in the CNS: congenital absence of CSF-1 in mice results in abnormal microglial response and increased neuron vulnerability to injury. Int. J. Dev. Neurosci. 13, 285–299.

Bonifer, C., Hume, D.A., 2008. The transcriptional regulation of the Colony-Stimulating Factor 1 Receptor (csf1r) gene during hematopoiesis. Front. Biosci. 13, 549–560.

Bosco, A., Crish, S.D., Steele, M.R., Romero, C.O., Inman, D.M., Horner, P.J., Calkins, D.J., Vetter, M.L., 2012. Early reduction of microglia activation by irradiation in a model of chronic glaucoma. PloS One 7, e43602.

Boyle, P., Levin, B., 2008. World Cancer Report 2008. IARC Press, Lyon.

Buffo, A., Vosko, M.R., Erturk, D., Hamann, G.F., Jucker, M., Rowitch, D., Gotz, M., 2005. Expression pattern of the transcription factor Olig2 in response to brain injuries: implications for neuronal repair. Proc. Natl. Acad. Sci. U. S. A. 102, 18183–18188.

Butovsky, O., Jedrychowski, M.P., Moore, C.S., Cialic, R., Lanser, A.J., Gabriely, G., Koeglsperger, T., Dake, B., Wu, P.M., Doykan, C.E., Fanek, Z., Liu, L., Chen, Z., Rothstein, J.D., Ransohoff, R.M., Gygi, S.P., Antel, J.P., Weiner, H.L., 2014. Identification of a unique TGF-beta-dependent molecular and functional signature in microglia. Nat. Neurosci. 17, 131–143.

Casey, A.E., Laster Jr., W.R., Ross, G.L., 1951. Sustained enhanced growth of carcinoma EO771 in C57 black mice. Proc. Soc. Exp. Biol. Med. 77, 358–362.

Celada, A., Borras, F.E., Soler, C., Lloberas, J., Klemsz, M., van Beveren, C., McKercher, S., Maki, R.A., 1996. The transcription factor PU.1 is involved in macrophage proliferation. J. Exp. Med. 184, 61–69.

Chen, H., Chong, Z.Z., De Toledo, S.M., Azzam, E.I., Elkabes, S., Souayah, N., 2016. Delayed activation of human microglial cells by high dose ionizing radiation. Brain Res. 1646, 193–198.

Chen, Z., Zhong, D., Li, G., 2019. The role of microglia in viral encephalitis: a review. J. Neuroinflammation 16, 76.

Chiang, C.S., McBride, W.H., Withers, H.R., 1993. Radiation-induced astrocytic and microglial responses in mouse brain. Radiother. Oncol. 29, 60–68.

Chihara, T., Suzu, S., Hassan, R., Chutiwitoonchai, N., Hiyoshi, M., Motoyoshi, K., Kimura, F., Okada, S., 2010. IL-34 and M-CSF share the receptor Fms but are not identical in biological activity and signal activation. Cell Death Differ. 17, 1917–1927.

Davalos, D., Grutzendler, J., Yang, G., Kim, J.V., Zuo, Y., Jung, S., Littman, D.R., Dustin, M.L., Gan, W.B., 2005. ATP mediates rapid microglial response to local brain injury in vivo. Nat. Neurosci. 8, 752–758.

Delaney, G., Jacob, S., Featherstone, C., Barton, M., 2005. The role of radiotherapy in cancer treatment: estimating optimal utilization from a review of evidence-based clinical guidelines. Cancer 104, 1129–1137.

DeSantis, C.E., Lin, C.C., Mariotto, A.B., Siegel, R.L., Stein, K.D., Kramer, J.L., Alteri, R., Robbins, A.S., Jemal, A., 2014. Cancer treatment and survivorship statistics, 2014. Ca - Cancer J. Clin. 64, 252–271.

Di Maggio, F.M., Minafra, L., Forte, G.I., Cammarata, F.P., Lio, D., Messa, C., Gilardi, M.C., Bravata, V., 2015. Portrait of inflammatory response to ionizing radiation treatment. J. Inflamm. 12, 14.

Elmore, M.R., Najafi, A.R., Koike, M.A., Dagher, N.N., Spangenberg, E.E., Rice, R.A., Kitazawa, M., Matusow, B., Nguyen, H., West, B.L., Green, K.N., 2014. Colony-stimulating factor 1 receptor signaling is necessary for microglia viability, unmasking a microglia progenitor cell in the adult brain. Neuron 82, 380–397.

Erblich, B., Zhu, L., Etgen, A.M., Dobrenis, K., Pollard, J.W., 2011. Absence of colony stimulation factor-1 receptor results in loss of microglia, disrupted brain development and olfactory deficits. PloS One 6, e26317.

Eriksson, D., Stigbrand, T., 2010. Radiation-induced cell death mechanisms. Tumour Biol. 31, 363–372.

Ewend, M.G., Elbabaa, S., Carey, L.A., 2005. Current treatment paradigms for the management of patients with brain metastases. Neurosurgery 57, S66–S77 discusssion S61-64.

Ewens, A., Mihich, E., Ehrke, M.J., 2005. Distant metastasis from subcutaneously grown E0771 medullary breast adenocarcinoma. Anticancer Res. 25, 3905–3915.

Eyo, U.B., Mo, M., Yi, M.H., Murugan, M., Liu, J., Yarlagadda, R., Margolis, D.J., Xu, P., Wu, L.J., 2018. P2Y12R-Dependent translocation mechanisms gate the changing microglial landscape. Cell Rep. 23, 959–966.

Fu, R.Y., Shen, Q.Y., Xu, P.F., Luo, J.J., Tang, Y.M., 2014. Phagocytosis of microglia in the central nervous system diseases. Mol. Neurobiol. 49, 1422–1434.
Gilmore, S.A., Phillips, N., Liu, K.M., Houle, J.D., 2003. Radiation-induced modulation of the microglial population in the normal and injured mature spinal cord. Exp. Neurol. 182, 169–179.
Ginhoux, F., Greter, M., Leboeuf, M., Nandi, S., See, P., Gokhan, S., Mehler, M.F., Conway, S.J., Ng, L.G., Stanley, E.R., Samokhvalov, I.M., Merad, M., 2010. Fate mapping analysis reveals that adult microglia derive from primitive macrophages. Science 330, 841–845.
Gomez-Nicola, D., Fransen, N.L., Suzzi, S., Perry, V.H., 2013. Regulation of microglial proliferation during chronic neurodegeneration. J. Neurosci. 33, 2481–2493.
Greene-Schloesser, D., Moore, E., Robbins, M.E., 2013. Molecular pathways: radiation-induced cognitive impairment. Clin. Canc. Res. 19, 2294–2300.
Greter, M., Lelios, I., Pelczar, P., Hoeffel, G., Price, J., Leboeuf, M., Kundig, T.M., Frei, K., Ginhoux, F., Merad, M., Becher, B., 2012. Stroma-derived interleukin-34 controls the development and maintenance of langerhans cells and the maintenance of microglia. Immunity 37, 1050–1060.
Guan, Z., Kuhn, J.A., Wang, X., Colquitt, B., Solorzano, C., Vaman, S., Guan, A.K., Evans-Reinsch, Z., Braz, J., Devor, M., Abboud-Werner, S.L., Lanier, L.L., Lomvardas, S., Basbaum, A.I., 2016. Injured sensory neuron-derived CSF1 induces microglial proliferation and DAP12-dependent pain. Nat. Neurosci. 19, 94–101.
Han, W., Umekawa, T., Zhou, K., Zhang, X.M., Ohshima, M., Dominguez, C.A., Harris, R.A., Zhu, C., Blomgren, K., 2016. Cranial irradiation induces transient microglia accumulation, followed by long-lasting inflammation and loss of microglia. Oncotarget 7, 82305–82323.
Haynes, S.E., Hollopeter, G., Yang, G., Kurpius, D., Dailey, M.E., Gan, W.B., Julius, D., 2006. The P2Y12 receptor regulates microglial activation by extracellular nucleotides. Nat. Neurosci. 9, 1512–1519.
Hua, K., Schindler, M.K., McQuail, J.A., Forbes, M.E., Riddle, D.R., 2012. Regionally distinct responses of microglia and glial progenitor cells to whole brain irradiation in adult and aging rats. PloS One 7, e52728.
Jeha, S., Pei, D., Choi, J., Cheng, C., Sandlund, J.T., Coustan-Smith, E., Campana, D., Inaba, H., Rubnitz, J.E., Ribeiro, R.C., Gruber, T.A., Raimondi, S.C., Khan, R.B., Yang, J.J., Mullighan, C.G., Downing, J.R., Evans, W.E., Relling, M.V., Pui, C.H., 2019. Improved CNS control of childhood acute lymphoblastic leukemia without cranial irradiation: St Jude total therapy study 16. J. Clin. Oncol. 37, 3377–3391.
Johnstone, C.N., Smith, Y.E., Cao, Y., Burrows, A.D., Cross, R.S., Ling, X., Redvers, R.P., Doherty, J.P., Eckhardt, B.L., Natoli, A.L., Restall, C.M., Lucas, E., Pearson, H.B., Deb, S., Britt, K.L., Rizzitelli, A., Li, J., Harmey, J.H., Pouliot, N., Anderson, R.L., 2015. Functional and molecular characterisation of EO771.LMB tumours, a new C57BL/6-mouse-derived model of spontaneously metastatic mammary cancer. Dis. Model. Mech. 8, 237–251.
Kalm, M., Lannering, B., Bjork-Eriksson, T., Blomgren, K., 2009. Irradiation-induced loss of microglia in the young brain. J. Neuroimmunol. 206, 70–75.
Kamphuis, W., Orre, M., Kooijman, L., Dahmen, M., Hol, E.M., 2012. Differential cell proliferation in the cortex of the APPswePS1dE9 Alzheimer's disease mouse model. Glia 60, 615–629.
Kyrkanides, S., Olschowka, J.A., Williams, J.P., Hansen, J.T., O'Banion, M.K., 1999. TNFα and IL-1β mediate intercellular adhesion molecule-1 induction via microglia–astrocyte interaction in CNS radiation injury. J. Neuroimmunol. 95, 95–106.
Lalancette-Hebert, M., Gowing, G., Simard, A., Weng, Y.C., Kriz, J., 2007. Selective ablation of proliferating microglial cells exacerbates ischemic injury in the brain. J. Neurosci. 27, 2596–2605.
Leibovich, S.J., Ross, R., 1975. The role of the macrophage in wound repair. A study with hydrocortisone and antimacrophage serum. Am. J. Pathol. 78, 71–100.
Li, T., Pang, S., Yu, Y., Wu, X., Guo, J., Zhang, S., 2013. Proliferation of parenchymal microglia is the main source of microgliosis after ischaemic stroke. Brain 136, 3578–3588.
Lin, H., Lee, E., Hestir, K., Leo, C., Huang, M., Bosch, E., Halenbeck, R., Wu, G., Zhou, A., Behrens, D., Hollenbaugh, D., Linnemann, T., Qin, M., Wong, J., Chu, K., Doberstein, S.K., Williams, L.T., 2008. Discovery of a cytokine and its receptor by functional screening of the extracellular proteome. Science 320, 807–811.
Lou, N., Takano, T., Pei, Y., Xavier, A.L., Goldman, S.A., Nedergaard, M., 2016. Purinergic receptor P2RY12-dependent microglial closure of the injured blood-brain barrier. Proc. Natl. Acad. Sci. U. S. A. 113, 1074–1079.
Manapov, F., Kasmann, L., Roengvoraphoj, O., Dantes, M., Schmidt-Hegemann, N.S., Belka, C., Eze, C., 2018. Prophylactic cranial irradiation in small-cell lung cancer: update on patient selection, efficacy and outcomes. Lung Canc. 9, 49–55.
Masteller, E.L., Wong, B.R., 2014. Targeting IL-34 in chronic inflammation. Drug Discov. Today 19, 1212–1216.
Menzel, F., Kaiser, N., Haehnel, S., Rapp, F., Patties, I., Schoneberg, N., Haimon, Z., Immig, K., Bechmann, I., 2018. Impact of X-irradiation on microglia. Glia 66, 15–33.
Mildenberger, M., Beach, T.G., Mcgeer, E.G., Ludgate, C.M., 1990. An animal-model of prophylactic cranial irradiation - histologic effects at acute, early and delayed stages. Int. J. Radiat. Oncol. Biol. Phys. 18, 1051–1060.
Mildner, A., Schmidt, H., Nitsche, M., Merkler, D., Hanisch, U.K., Mack, M., Heikenwalder, M., Bruck, W., Priller, J., Prinz, M., 2007. Microglia in the adult brain arise from Ly-6ChiCCR2+ monocytes only under defined host conditions. Nat. Neurosci. 10, 1544–1553.
Mizumatsu, S., Monje, M.L., Morhardt, D.R., Rola, R., Palmer, T.D., Fike, J.R., 2003. Extreme sensitivity of adult neurogenesis to low doses of X-irradiation. Canc. Res. 63, 4021–4027.
Mizuno, T., Doi, Y., Mizoguchi, H., Jin, S., Noda, M., Sonobe, Y., Takeuchi, H., Suzumura, A., 2011. Interleukin-34 selectively enhances the neuroprotective effects of microglia to attenuate oligomeric amyloid-beta neurotoxicity. Am. J. Pathol. 179, 2016–2027.
Monje, M.L., Mizumatsu, S., Fike, J.R., Palmer, T.D., 2002. Irradiation induces neural precursor-cell dysfunction. Nat. Med. 8, 955–962.
Moravan, M.J., Olschowka, J.A., Williams, J.P., O'Banion, M.K., 2011. Cranial irradiation leads to acute and persistent neuroinflammation with delayed increases in T-cell infiltration and CD11c expression in C57BL/6 mouse brain. Radiat. Res. 176, 459–473.
Moravan, M.J., Olschowka, J.A., Williams, J.P., O'Banion, M.K., 2016. Brain radiation injury leads to a dose- and time-dependent recruitment of peripheral myeloid cells that depends on CCR2 signaling. J. Neuroinflammation 13, 30.
Okubo, M., Yamanaka, H., Kobayashi, K., Dai, Y., Kanda, H., Yagi, H., Noguchi, K., 2016. Macrophage-colony stimulating factor derived from injured primary afferent induces proliferation of spinal microglia and neuropathic pain in rats. PloS One 11, e0153375.
Olmos-Alonso, A., Schetters, S.T., Sri, S., Askew, K., Mancuso, R., Vargas-Caballero, M., Holscher, C., Perry, V.H., Gomez-Nicola, D., 2016. Pharmacological targeting of CSF1R inhibits microglial proliferation and prevents the progression of Alzheimer's-like pathology. Brain 139, 891–907.
Oosterhof, N., Kuil, L.E., van der Linde, H.C., Burm, S.M., Berdowski, W., van Ijcken, W.F.J., van Swieten, J.C., Hol, E.M., Verheijen, M.H.G., van Ham, T.J., 2018. Colony-stimulating factor 1 receptor (CSF1R) regulates microglia density and distribution, but not microglia differentiation in vivo. Cell Rep. 24, 1203–1217 e1206.
Prise, K.M., Schettino, G., Folkard, M., Held, K.D., 2005. New insights on cell death from radiation exposure. Lancet Oncol. 6, 520–528.
Raivich, G., Haas, S., Werner, A., Klein, M.A., Kloss, C., Kreutzberg, G.W., 1998. Regulation of MCSF receptors on microglia in the normal and injured mouse central nervous system: a quantitative immunofluorescence study using confocal laser microscopy. J. Comp. Neurol. 395, 342–358.
Raivich, G., Moreno-Flores, M.T., Moller, J.C., Kreutzberg, G.W., 1994. Inhibition of posttraumatic microglial proliferation in a genetic model of macrophage colony-stimulating factor deficiency in the mouse. Eur. J. Neurosci. 6, 1615–1618.
Rice, R.A., Pham, J., Lee, R.J., Najafi, A.R., West, B.L., Green, K.N., 2017. Microglial repopulation resolves inflammation and promotes brain recovery after injury. Glia 65, 931–944.
Roesch, S., Rapp, C., Dettling, S., Herold-Mende, C., 2018. When immune cells turn bad-tumor-associated microglia/macrophages in glioma. Int. J. Mol. Sci. 19, 436.
Rola, R., Otsuka, S., Obenaus, A., Nelson, G.A., Limoli, C.L., VandenBerg, S.R., Fike, J.R., 2004a. Indicators of hippocampal neurogenesis are altered by 56Fe-particle irradiation in a dose-dependent manner. Radiat. Res. 162, 442–446.
Rola, R., Raber, J., Rizk, A., Otsuka, S., VandenBerg, S.R., Morhardt, D.R., Fike, J.R., 2004b. Radiation-induced impairment of hippocampal neurogenesis is associated with cognitive deficits in young mice. Exp. Neurol. 188, 316–330.
Slotman, B., Faivre-Finn, C., Kramer, G., Rankin, E., Snee, M., Hatton, M., Postmus, P., Collette, L., Musat, E., Senan, S., Group, E.R.O., Lung Cancer, G., 2007. Prophylactic cranial irradiation in extensive small-cell lung cancer. N. Engl. J. Med. 357, 664–672.
Snyder, J.S., Hong, N.S., McDonald, R.J., Wojtowicz, J.M., 2005. A role for adult neurogenesis in spatial long-term memory. Neuroscience 130, 843–852.
Sweet, T.B., Hurley, S.D., Wu, M.D., Olschowka, J.A., Williams, J.P., O'Banion, M.K., 2016. Neurogenic effects of low-dose whole-body HZE (Fe) ion and gamma irradiation. Radiat. Res. 186, 614–623.
Sweet, T.B., Panda, N., Hein, A.M., Das, S.L., Hurley, S.D., Olschowka, J.A., Williams, J.P., O'Banion, M.K., 2014. Central nervous system effects of whole-body proton irradiation. Radiat. Res. 182, 18–34.
Swiatkowski, P., Murugan, M., Eyo, U.B., Wang, Y., Rangaraju, S., Oh, S.B., Wu, L.J., 2016. Activation of microglial P2Y12 receptor is required for outward potassium currents in response to neuronal injury. Neuroscience 318, 22–33.
Takeuchi, A., Miyaishi, O., Kiuchi, K., Isobe, K., 2001. Macrophage colony-stimulating factor is expressed in neuron and microglia after focal brain injury. J. Neurosci. Res. 65, 38–44.
Tremblay, M.E., Stevens, B., Sierra, A., Wake, H., Bessis, A., Nimmerjahn, A., 2011. The role of microglia in the healthy brain. J. Neurosci. 31, 16064–16069.
Udovicich, C., Phillips, C., Kok, D.L., Tange, D., Plumridge, N.M., Prabhu, R.S., Haghighi, N., 2019. Neoadjuvant stereotactic radiosurgery: a further evolution in the management of brain metastases. Curr. Oncol. Rep. 21, 73.
van Furth, R., Cohn, Z.A., 1968. The origin and kinetics of mononuclear phagocytes. J. Exp. Med. 128, 415–435.
Varvel, N.H., Grathwohl, S.A., Baumann, F., Liebig, C., Bosch, A., Brawek, B., Thal, D.R., Charo, I.F., Heppner, F.L., Aguzzi, A., Garaschuk, O., Ransohoff, R.M., Jucker, M., 2012. Microglial repopulation model reveals a robust homeostatic process for replacing CNS myeloid cells. Proc. Natl. Acad. Sci. U. S. A. 109, 18150–18155.
Wang, Y., Colonna, M., 2014. Interkeukin-34, a cytokine crucial for the differentiation and maintenance of tissue resident macrophages and Langerhans cells. Eur. J. Immunol. 44, 1575–1581.
Williams, J.P., Calvi, L., Chakkalakal, J.V., Finkelstein, J.N., O'Banion, M.K., Puzas, E., 2016. Addressing the symptoms or fixing the problem? Developing countermeasures against normal tissue radiation injury. Radiat. Res. 186, 1–16.
Xu, J., Escamilla, J., Mok, S., David, J., Priceman, S., West, B., Bollag, G., McBride, W., Wu, L., 2013. CSF1R signaling blockade stanches tumor-infiltrating myeloid cells and improves the efficacy of radiotherapy in prostate cancer. Canc. Res. 73, 2782–2794.
Xue, J., Dong, J.H., Huang, G.D., Qu, X.F., Wu, G., Dong, X.R., 2014. NF-kappaB signaling modulates radiationinduced microglial activation. Oncol. Rep. 31, 2555–2560.
Yamamoto, S., Kohsaka, S., Nakajima, K., 2012. Role of cell cycle-associated proteins in microglial proliferation in the axotomized rat facial nucleus. Glia 60, 570–581.

Yamamoto, S., Nakajima, K., Kohsaka, S., 2010. Macrophage-colony stimulating factor as an inducer of microglial proliferation in axotomized rat facial nucleus. J. Neurochem. 115, 1057–1067.

Yin, X., Yan, D., Qiu, M., Huang, L., Yan, S.X., 2019. Prophylactic cranial irradiation in small cell lung cancer: a systematic review and meta-analysis. BMC Canc. 19, 95.

Yona, S., Kim, K.W., Wolf, Y., Mildner, A., Varol, D., Breker, M., Strauss-Ayali, D., Viukov, S., Guilliams, M., Misharin, A., Hume, D.A., Perlman, H., Malissen, B., Zelzer, E., Jung, S., 2013. Fate mapping reveals origins and dynamics of monocytes and tissue macrophages under homeostasis. Immunity 38, 79–91.

Zhang, P., Behre, G., Pan, J., Iwama, A., Wara-Aswapati, N., Radomska, H.S., Auron, P.E., Tenen, D.G., Sun, Z., 1999. Negative cross-talk between hematopoietic regulators: GATA proteins repress PU.1. Proc. Natl. Acad. Sci. U. S. A. 96, 8705–8710.

Zhang, Y., Chen, K., Sloan, S.A., Bennett, M.L., Scholze, A.R., O'Keeffe, S., Phatnani, H.P., Guarnieri, P., Caneda, C., Ruderisch, N., Deng, S., Liddelow, S.A., Zhang, C., Daneman, R., Maniatis, T., Barres, B.A., Wu, J.Q., 2014. An RNA-sequencing transcriptome and splicing database of glia, neurons, and vascular cells of the cerebral cortex. J. Neurosci. 34, 11929–11947.

Zhou, K., Bostrom, M., Ek, C.J., Li, T., Xie, C., Xu, Y., Sun, Y., Blomgren, K., Zhu, C., 2017. Radiation induces progenitor cell death, microglia activation, and blood-brain barrier damage in the juvenile rat cerebellum. Sci. Rep. 7, 46181.

Zhu, W., Umegaki, H., Shinkai, T., Kurotani, S., Suzuki, Y., Endo, H., Iguchi, A., 2003. Different glial reactions to hippocampal stab wounds in young adult and aged rats. J. Gerontol. Biol. Med. Sci. 58, 117–122.